

Electron self-trapping on a nano-circle

L.S. Brizhik*, and A.A. Eremko†

Bogolyubov Institute for Theoretical Physics, 03143 Kyiv, Ukraine

B. Piette‡ and W. Zakrzewski§

Department of Mathematical Sciences, University of Durham,
Durham DH1 3LE, UK

Abstract

We study the self-trapping of quasiparticles (electrons, holes, excitons, etc) in a molecular chain with the structure of a ring, taking into account the electron-phonon interaction and the radial and tangential deformations of the chain. A discrete system of equations is obtained and solved numerically. The analytical solutions for the wave function of a quasiparticle and for the molecule displacements that determine the distortion of the ring, are also obtained and solved in the continuum approximation. The numerical solutions of the system of discrete nonlinear equations reveals several regimes of quasiparticle localisation in the chain which depend on the values of the parameters of the system. It is shown that the transversal deformation of the chain favours the formation of a soliton.

1 Introduction.

The study of various physical properties of carbon nanotubes has received a lot of attention during the last few years. In particular, B. Hartmann et al [1] have recently studied the electron-phonon interaction on a hexagonal lattice. Their approach was, however, limited in its scope as it did not take

*e-mail address: brizhik@bitp.kiev.ua

†e-mail address: eremko@bitp.kiev.ua

‡e-mail address: B.M.A.G.Piette@durham.ac.uk

§e-mail address: W.J.Zakrzewski@durham.ac.uk

into account the possible displacement of atoms in the direction perpendicular to the nanotube. To address this problem, we have to introduce three phonon fields, two of which are tangent to the tube while the third one is perpendicular to it. The introduction of such a transversal field is not very straightforward. It requires the generalization of the phonon Hamiltonian to describe the bending elasticity of the tube. Such a generalization is presented in this paper for the case of a nanocircle. A study of the electron-phonon interaction in a simple model where such a transversal field is introduced, paves the way towards the study of a more relevant model describing carbon nanotubes. It also describes various physical properties, including the conductivity and conformational states, of other physical systems such as circular macromolecules, cyclic organic, inorganic and semi-inorganic polymeric macromolecules.

Our model describes a circular closed chain of monomers which are allowed to move in the plane spanned by the circle at rest. Thus, it is a two-dimensional model where deformations in the direction perpendicular to the circle plane, are not allowed. One can think of this model as a crude cross section of a carbon nanotube, though obviously, the hexagonal symmetry of the carbon nanotube, and its three-dimensional nature require a more general description. Nevertheless, our hope is to gain some understanding of how one can take into account the transversal displacement of atoms.

At the same time, our model does describe real physical low-dimensional cyclic nanosystems that include a large class of end-linked natural and synthetic low-dimensional macromolecules and nanosystems with a circular structure. Amongst them one finds the cyclic biological macromolecules, such as intact DNA from most prokaryotes and viruses, mitochondria plasmid DNA [2, 3, 4], cyclic DNA macroarrays used for the systematic screening of gene expression [5, 6, 7]. Large circular single stranded RNAs form genomic material of viroids [8, 9]. Some of the oligoribonucleotides with known biological activity are also cyclic molecules [10, 11, 12, 13]. The so called “second messengers” also have a circular structure. Amongst them are the messengers which regulate the channels involved in the initiation of impulses in neurons responding to odors and light, messengers which function as calcium regulated transcription factors or as a substrate for depolarization-activated calcium calmodulin-dependent protein kinases I and II (e.g., cAMP Response Element-Binding Protein, known also as CREB protein) [14]. In addition, there are also messengers which induce and control transcription from the proximal promoter of the human aromatase responsible for the metabolism of steroids [15]. Therefore, our study of distortions of molecular

nano-circles due to electron-phonon coupling could bring some insight into the structure-function relationship of biological macromolecules.

End-linked organic, inorganic and semi-inorganic polymers are now known as functional materials with applications as biologically active species, catalyst supports, charge carriers etc. For instance, the long-chain circular esters are used for soft lenses, cyclic trimeric phosphazene rings are valuable technological materials for their high heat resistance and flame retardant behaviour. Polysiloxanes, which are the main components of silicone products, are one of the most important cyclic materials ([16] and references cited therein).

The circular structure of these macromolecules, their relative softness, deformability and ability to form cross-linking suggest modelling such systems by a nanocircle of periodically placed monomers of a given length. Under certain conditions one or several monomers of the nanocircle can be excited by an external field (light or electromagnetic radiation, trapping of extra electron or hole, etc.). Such an excitation, called in what follows, a quasiparticle, can move onto the neighbouring monomers and cause a local distortion of the ring due to the electron-phonon coupling. In a linear chain it can lead to the change of properties of the quasiparticle, depending on the strength of the coupling. At weak coupling the quasiparticle remains almost free, at strong coupling it is trapped on one site (a small polaron is formed), while at intermediate values of the coupling a self-trapping occurs within few lattice sites and a nonlinear soliton-like state is formed [17, 18, 19]. It turns out that the physical properties of systems at different regimes of localisation differ significantly, and, therefore, the classification of systems by their electron ground states is important.

One can expect that, depending on the strength of the electron-phonon coupling, similar regimes take place in a very large end-linked circle. However, this is not clear for a circle of a finite and not very large length. This problem is studied in the present paper. We start by deriving a Hamiltonian describing the elastic properties of a nanocircle and a Hamiltonian describing the interaction between the electron and the phonon fields. We then derive the corresponding system of discrete equations and compute solutions for this model. We show that the model exhibits several classes of solutions depending on the values of the parameters. In particular, we show that the electron-phonon interaction leads to the self-trapping of a quasiparticle and introduces a deformation of the chain.

2 The nano-circle

We consider a molecular chain which consists of periodically repeated units (atoms or groups of atoms) bound by chemical or hydrogen bonds. We assume that these bonds between the units are directed in such a way that, for a molecular chain with free ends, the minimum of the free energy corresponds to a linear one-dimensional structure in which chain sites are placed at the equilibrium distance a_0 and all intersite bonds are directed along the chain axis.

We focus our attention on a study of the molecular chain which is closed to form a circle (before any deformations are allowed). The equilibrium positions of the chain sites are determined by the radius-vectors

$$\vec{R}_n^{(0)} = R_0[\vec{e}_x \sin(n\alpha + \theta_0) + \vec{e}_y \cos(n\alpha + \theta_0)] \quad (1)$$

where the centre of the coordinate system is placed at the centre of the circle, R_0 is the circle radius, $n = 1, \dots, N$ enumerates the chain sites, $\alpha = 2\pi/N$ where N is the number of sites in the ring, and θ_0 is an arbitrary angle. The equilibrium distance between the sites in the molecular circle is

$$D_{n,n+1}^{(0)} = |\vec{D}_{n,n+1}^{(0)}| = |\vec{R}_{n+1}^{(0)} - \vec{R}_n^{(0)}| = 2R_0 \sin\left(\frac{\alpha}{2}\right) = a \quad (2)$$

which, in general, can differ from a_0 . Thus, the radius of the circle is $R_0 = a/(2 \sin(\frac{\alpha}{2}))$. Note that if there is a bending of chemical bonds at each site n , this bending can be described by the angle $\beta_n^{(0)}$ between the vectors $\vec{D}_{n-1,n}^{(0)} = \vec{R}_n^{(0)} - \vec{R}_{n-1}^{(0)}$ and $\vec{D}_{n,n+1}^{(0)} = \vec{R}_{n+1}^{(0)} - \vec{R}_n^{(0)}$:

$$\cos \beta_n^{(0)} = \frac{(\vec{D}_{n-1,n}^{(0)} \cdot \vec{D}_{n,n+1}^{(0)})}{|\vec{D}_{n-1,n}^{(0)}| |\vec{D}_{n,n+1}^{(0)}|} = \cos(\alpha), \quad (3)$$

i.e., $\beta_n^{(0)} = \alpha$.

Due to the displacements the real positions of the sites are

$$\vec{R}_n = \vec{R}_n^{(0)} + \vec{r}_n, \quad (4)$$

where \vec{r}_n is the displacement of the site n from the equilibrium position. Note that we can represent the vector \vec{r}_n using the following orthogonal unit vectors $\vec{e}_n^{(r)}$ and $\vec{e}_n^{(t)}$

$$\vec{e}_n^{(t)} = \vec{e}_x \cos(n\alpha + \theta_0) - \vec{e}_y \sin(n\alpha + \theta_0), \quad (5)$$

$$\vec{e}_n^{(r)} = \vec{e}_x \sin(n\alpha + \theta_0) + \vec{e}_y \cos(n\alpha + \theta_0). \quad (6)$$

We then have

$$\vec{r}_n = \vec{e}_n^{(t)} r_{t,n} + \vec{e}_n^{(r)} r_{r,n}, \quad (7)$$

where $r_{t,n} \equiv u_n$ is the displacement tangential to the circle while $r_{r,n} \equiv s_n$ is the displacement perpendicular to the circle (the tangential and radial components of displacement respectively). Thus the real distances between the sites and the bending angles differ from their equilibrium values: $D_{n,n+1} = a + d_{n,n+1}$ and $\beta_n = \alpha + \Delta\beta_n$.

The vector, which links the site n with the $n + 1$ one, is $\vec{D}_{n,n+1} = \vec{R}_{n+1} - \vec{R}_n = \vec{D}_{n,n+1}^{(0)} + \vec{d}_{n,n+1}$ where $\vec{d}_{n,n+1} = \vec{r}_{n+1} - \vec{r}_n$. So, the distance is given by

$$D_{n,n+1} = |\vec{D}_{n,n+1}| = \sqrt{(\vec{D}_{n,n+1}^{(0)} + \vec{d}_{n,n+1})^2} \approx a + \frac{(\vec{D}_{n,n+1}^{(0)} \cdot \vec{d}_{n,n+1})}{a} = a + U_n, \quad (8)$$

where

$$U_n = \cos\left(\frac{\alpha}{2}\right)(u_{n+1} - u_n) + \sin\left(\frac{\alpha}{2}\right)(s_n + s_{n+1}). \quad (9)$$

To obtain this expression we have assumed that the relative site displacements are small, i.e. $|\vec{d}_{i,i+1}|^2 \ll a^2$. In this case the deviations of the bending angles from their equilibrium values are also small, and we can write

$$\begin{aligned} \cos(\beta_n) &= \cos(\alpha + \Delta\beta_n) \\ &= \cos(\alpha) \cos(\Delta\beta_n) - \sin(\alpha) \sin(\Delta\beta_n) \approx \cos(\alpha) - \sin(\alpha)(\Delta\beta_n). \end{aligned} \quad (10)$$

For $\cos(\beta_n)$ we can put

$$\begin{aligned} \cos \beta_n &= \frac{(\vec{D}_{n-1,n} \cdot \vec{D}_{n,n+1})}{|\vec{D}_{n-1,n}| |\vec{D}_{n,n+1}|} \\ &\approx \frac{(\vec{D}_{n-1,n}^{(0)} \cdot \vec{D}_{n,n+1}^{(0)}) + (\vec{D}_{n-1,n}^{(0)} \cdot \vec{d}_{n,n+1}) + (\vec{D}_{n,n+1}^{(0)} \cdot \vec{d}_{n-1,n})}{(a + U_{n-1})(a + U_n)} \\ &\approx \cos \alpha - \sin \alpha \left(\sin \frac{\alpha}{2} \frac{u_{n+1} - u_{n-1}}{a} + \cos \frac{\alpha}{2} \frac{2s_n - s_{n+1} - s_{n-1}}{a} \right). \end{aligned} \quad (11)$$

Thus, we have arrived at the following expression for $\Delta\beta_n$:

$$\Delta\beta_n = \frac{A_n}{a}, \quad (12)$$

where

$$A_n = \sin \frac{\alpha}{2} (u_{n+1} - u_{n-1}) + \cos \frac{\alpha}{2} (2s_n - s_{n+1} - s_{n-1}). \quad (13)$$

3 The Hamiltonian

Next, we assume that the individual isolated monomers are characterised by nondegenerate electronic excitations with energy E_0 . In the approximation of the nearest neighbour interaction, the total Hamiltonian which describes the electronic excitations (or, in the tight binding approximation, the additional electrons) and harmonic vibrations in a molecular chain can be written as

$$H = \sum_n \left(\mathcal{E}_n B_n^\dagger B_n - J_{n,n+1} (B_n^\dagger B_{n+1} + B_{n+1}^\dagger B_n) \right) + H_{ph}, \quad (14)$$

where B_n^\dagger , B_n are the creation and annihilation operators of the quasiparticle at the n -th site of the circle, $\mathcal{E}_n = E_0 + V_n$ is the on-site electron energy, where V_n is the change of the electron energy due to the influence of the neighbouring sites. Furthermore, $J_{n,n+1}$ describes the quasiparticle transfer between the nearest neighbours, and H_{ph} is the Hamiltonian of the site displacements. The electron-phonon interaction is determined by the dependence of V_n and $J_{n,n+1}$ on the positions of the neighbours of the n -th site. The term $J_{n,n+1}$ depends on the distance between the sites $D_{n,n+1} = a + U_n$ and, within the linear approximation with respect to the displacements, we can put it as

$$J_{n,n+1} = J - G_2 U_n, \quad (15)$$

where $J = J(a)$ and $G_2 = -dJ/da$.

V_n is determined by the influence of the neighbours; thus it depends on the distance between them and on the bending angle of the chemical bonds: $V_n = V_{n-1,n}(a + U_{n-1}) + V_{n,n+1}(a + U_n) + V_n(\beta_n)$. Hence the on-site electron energy, within the displacements' linear approximation, can be written as

$$\begin{aligned} \mathcal{E}_n &= \mathcal{E}_0 + \chi_1 (U_n + U_{n-1}) + \chi_2 A_n \\ &= \mathcal{E}_0 + \left(\chi_1 \cos \frac{\alpha}{2} + \chi_2 \sin \frac{\alpha}{2} \right) (u_{n+1} - u_{n-1}) + 2 \left(\chi_1 \sin \frac{\alpha}{2} + \chi_2 \cos \frac{\alpha}{2} \right) s_n \\ &\quad + \left(\chi_1 \sin \frac{\alpha}{2} - \chi_2 \cos \frac{\alpha}{2} \right) (s_{n+1} + s_{n-1}), \end{aligned} \quad (16)$$

where $\chi_1 = dV_{n\pm 1,n}(a)/da$, $\chi_2 = (1/a)dV_n(\beta_n)/d\beta_n|_{\beta_n=\alpha}$. The parameters χ_1 , χ_2 and G_2 determine the interaction of the quasiparticle with the chain deformation (exciton/electron-phonon coupling) in the linear approximation relative to the site displacements from their equilibrium positions.

Due to the symmetry we see that $V_n(\beta_n) = V_n(-\beta_n)$, and we can set $V_n(\beta_n) = V_n(\cos(\beta_n))$. Therefore,

$$\chi_2 = (1/a) \frac{dV_n(\beta_n)}{d\beta_n} \Big|_{\beta_n=\alpha} = -(1/a) V_n' \sin(\alpha). \quad (17)$$

Thus, $\chi_2 \sim \sin(\alpha)$ and $\chi_2 = 0$ at $\alpha = 0$ and in the linear chain the expansion of $V_n(\beta_n)$ in series of $\Delta\beta_n$ begins with the quadratic term while the linear term vanishes.

The Hamiltonian of the site displacements, H_{ph} , consists of the kinetic and potential energies of displacements. The potential energy consists of the potential energies of the pairwise interactions, which depend on the distance between the sites, and on the bending contribution. Therefore, the total Hamiltonian of the phonons takes the form:

$$H_{ph} = \frac{1}{2} \sum_n \left(\frac{\vec{p}_n^2}{M} + \kappa (|\vec{R}_{n+1} - \vec{R}_n| - a_0)^2 + \kappa_b a_0^2 (\beta_n - \beta_0)^2 \right). \quad (18)$$

Here M is the mass of a lattice site, \vec{p}_n are the momentum operators canonically conjugate to the operators of displacements \vec{r}_n , κ is the elasticity coefficient due to the change of distance between the molecules from their equilibrium value a_0 , and κ_b is the elasticity constant responsible for the bending of the bond (for small bending angles β_n).

As our chain is closed to form a circle, we have $\beta_n = \alpha + \Delta\beta_n = \alpha + aA_n$. From the definition of A_n we see that $\sum_n A_n = 0$ and, therefore, the equilibrium distance between the lattice sites on the circle remains the same: $a = a_0$. Therefore, the total Hamiltonian for phonons in a circle takes the form:

$$\begin{aligned} H_{ph} &= \frac{1}{2} \sum_n \left(\frac{p_n^2}{M} + \frac{q_n^2}{M} + \kappa \left[\cos\left(\frac{\alpha}{2}\right)(u_{i+1} - u_i) + \sin\left(\frac{\alpha}{2}\right)(s_i + s_{i+1}) \right]^2 \right. \\ &\quad \left. + \kappa_b \left(\sin\frac{\alpha}{2}(u_{n+1} - u_{n-1}) + \cos\frac{\alpha}{2}(2s_n - s_{n+1} - s_{n-1}) \right)^2 \right) + \mathcal{W}_b \\ &= \frac{1}{2} \sum_n \left(\frac{p_n^2}{M} + \frac{q_n^2}{M} + \kappa U_n^2 + \kappa_b A_n^2 \right) + \mathcal{W}_b, \end{aligned} \quad (19)$$

where p_n and q_n are the momentum operators canonically conjugate to the operators of the tangential and radial components of the site displacements, respectively, and $\mathcal{W}_b = (1/2)\kappa_b a^2 \alpha^2 N = 2\pi^2 \kappa_b a^2 / N$ is the energy required to bend the linear chain into a circle (which we will drop from now on as it is a constant).

Note that both U_n and A_n are invariant under the global translations of the circle and so is the Hamiltonian (19), as one would expect.

Thus, the total Hamiltonian is given by

$$H = H_e + H_{ph} + H_{int}, \quad (20)$$

where

$$H_e = \sum_n \left(\mathcal{E}_0 B_n^\dagger B_n - J (B_n^\dagger B_{n+1} + B_{n+1}^\dagger B_n) \right), \quad (21)$$

$$H_{int} = \sum_n \left(B_n^\dagger B_n [\chi_1 (U_n + U_{n-1}) + \chi_2 A_n] + G_2 (B_n^\dagger B_{n+1} + B_{n+1}^\dagger B_n) U_n \right), \quad (22)$$

and H_{ph} is given by (19).

These expressions are written in the site representation. We can transform them into the quasimomentum representation by performing the unitary transformation

$$B_n = \frac{1}{\sqrt{N}} \sum_k e^{ikn} B_k, \quad (23)$$

$$\begin{aligned} u_n &= \frac{1}{\sqrt{MN}} \sum_q e^{iqn} U_{l,q}, & p_n &= \sqrt{\frac{M}{N}} \sum_q e^{-iqn} \Pi_{l,q}, \\ s_n &= \frac{1}{\sqrt{MN}} \sum_q e^{iqn} U_{r,q}, & q_n &= \sqrt{\frac{M}{N}} \sum_q e^{-iqn} \Pi_{r,q}, \end{aligned} \quad (24)$$

where k (or q) = $2\pi\nu/N$, $\nu = 0, \pm 1, \dots, \pm(N/2 - 1), N/2$ for N even and $\nu = 0, \pm 1, \dots, \pm(N - 1)/2$ for N odd. This allows us to rewrite the quasiparticle Hamiltonian (21) and the phonon Hamiltonian (19) as

$$H_e = \sum_k \mathcal{E}(k) B_k^\dagger B_k, \quad (25)$$

$$H_{ph} = \frac{1}{2} \sum_q \left(\sum_\mu (\Pi_{\mu,q}^\dagger \Pi_{\mu,q} + \omega_\mu^2(q) U_{\mu,q}^\dagger U_{\mu,q}) + if(q) (U_{r,q}^\dagger U_{l,q} - U_{l,q}^\dagger U_{r,q}) \right), \quad (26)$$

where $\mu = l, r$, and

$$\mathcal{E}(k) = \mathcal{E}_0 - 2J \cos(k), \quad (27)$$

$$\begin{aligned}
\omega_l^2(q) &= 4\frac{\kappa}{M}\sin^2\left(\frac{q}{2}\right)\left[\cos^2\left(\frac{\alpha}{2}\right) + 4c\sin^2\left(\frac{\alpha}{2}\right)\cos^2\left(\frac{q}{2}\right)\right], \\
\omega_r^2(q) &= 4\frac{\kappa}{M}\left[\sin^2\left(\frac{\alpha}{2}\right)\cos^2\left(\frac{q}{2}\right) + 4c\cos^2\left(\frac{\alpha}{2}\right)\sin^4\left(\frac{q}{2}\right)\right], \\
f(q) &= \frac{\kappa}{M}\sin(\alpha)\sin(q)\left[1 + 4c\sin^2\left(\frac{q}{2}\right)\right].
\end{aligned} \tag{28}$$

Here $c = \kappa_b/\kappa$.

Applying the unitary canonical transformation

$$\begin{aligned}
U_{l,q} &= \cos(\theta(q))Q_{1,q} + i\sin(\theta(q))Q_{2,q}, & \Pi_{l,q} &= \cos(\theta(q))P_{1,q} - i\sin(\theta(q))P_{2,q}, \\
U_{r,q} &= i\sin(\theta(q))Q_{1,q} + \cos(\theta(q))Q_{2,q}, & \Pi_{r,q} &= -i\sin(\theta(q))P_{1,q} + \cos(\theta(q))P_{2,q},
\end{aligned} \tag{29}$$

in which

$$\tan(2\theta(q)) = \frac{2f(q)}{\Delta(q)}, \quad \Delta(q) = \omega_l^2(q) - \omega_r^2(q), \tag{30}$$

we obtain the phonon Hamiltonian in the diagonal form

$$H_{ph} = \frac{1}{2} \sum_{j,q} \left(P_{j,q}^\dagger P_{j,q} + \Omega_j^2(q) Q_{j,q}^\dagger Q_{j,q} \right), \tag{31}$$

where $j = 1, 2$ and

$$\Omega_j^2(q) = \frac{1}{2} \left(\omega_l^2(q) + \omega_r^2(q) - (-1)^j [(\omega_l^2(q) - \omega_r^2(q)) \cos(2\theta(q)) + 2f(q) \sin(2\theta(q))] \right). \tag{32}$$

Then we can introduce the operators of creation $b_{q,j}^\dagger$ and annihilation $b_{q,j}$ of phonons by performing a further canonical transformation

$$Q_{j,q} = \sqrt{\frac{\hbar}{2\Omega_j(q)}} (b_{q,j} + b_{-q,j}^\dagger), \tag{33}$$

$$P_{j,q} = -i\sqrt{\frac{\hbar\Omega_j(q)}{2}} (b_{q,j} - b_{-q,j}^\dagger), \tag{34}$$

and find that the total Hamiltonian can be rewritten as

$$H = \sum_k \mathcal{E}(k) B_k^\dagger B_k + \sum_{j,q} \hbar\Omega_j(q) \left(b_{q,j}^\dagger b_{q,j} + \frac{1}{2} \right) + \tag{35}$$

$$+ \frac{1}{\sqrt{MN}} \sum_{k,q,j} \Phi_j(k, q) B_{k+q}^\dagger B_k (b_{q,j} + b_{-q,j}^\dagger) \tag{36}$$

where the coupling functions $\Phi_j(k, q)$ are given by

$$\Phi_j(k, q) = F_j(k, q) \sqrt{\frac{\hbar}{2\Omega_j(q)}} \quad (37)$$

with

$$\begin{aligned} F_1(k, q) &= 4i[F_l(k, q) \cos(\theta(q)) + F_r(k, q) \sin(\theta(q))], \\ F_2(k, q) &= 4[F_r(k, q) \cos(\theta(q)) - F_l(k, q) \sin(\theta(q))]. \end{aligned} \quad (38)$$

Here

$$\begin{aligned} F_l(k, q) &= [(\chi_1 \cos(\frac{\alpha}{2}) + \chi_2 \sin(\frac{\alpha}{2})) \cos(\frac{q}{2}) + G_2 \cos(\frac{\alpha}{2}) \cos(k + \frac{q}{2})] \sin(\frac{q}{2}), \\ F_r(k, q) &= \chi_1 \sin(\frac{\alpha}{2}) \cos^2(\frac{q}{2}) + \chi_2 \cos(\frac{\alpha}{2}) \sin^2(\frac{q}{2}) + G_2 \sin(\frac{\alpha}{2}) \cos(k + \frac{q}{2}) \cos(\frac{q}{2}). \end{aligned} \quad (39)$$

Note that $\Phi_j^*(k, q) = \Phi_j(k + q, -q)$.

At large values of N the parameter α is small ($N \rightarrow \infty$, $\alpha \rightarrow 0$). At $\alpha = 0$ we have a linear molecular chain. In this case, according to (28), $f(q) = 0$ and the longitudinal $Q_{1,q} = U_{l,q}$ (along the chain axis) and the transversal $Q_{2,q} = U_{r,q}$ displacements do not mix ($\theta(q) = 0$ in (29)). A linear chain is characterised by the longitudinal acoustic waves $U_{l,q}$ with frequency

$$\omega_l^2(q) = 4 \frac{\kappa}{M} \sin^2(\frac{q}{2}), \quad (40)$$

and the bending waves $U_{r,q}$ with frequency

$$\omega_r^2(q) = 16 \frac{\kappa_b}{M} \sin^4(\frac{q}{2}). \quad (41)$$

In a linear chain in the linear approximation with regard to the displacements, quasiparticles interact only with the longitudinal acoustic phonons because

$$F_1(k, q) = 4iF_l(k, q) = 4i[(\chi_1 \cos(\frac{q}{2}) + G_2 \cos(k + \frac{q}{2})) \sin(\frac{q}{2})] \quad (42)$$

and $F_2(k, q) = 4F_r(k, q) = 4\chi_2 \sin^2(\frac{q}{2}) = 0$ (as $\chi_2 \sim \sin(\alpha)$ and so $\chi_2 = 0$ at $\alpha = 0$).

Note that in a long linear chain, N which is included in the definition of the one-dimensional quasimomentum q , determines the main region of

quantization. So, we have $q = 2\pi\nu/N = \alpha\nu$, $\nu = 0, \pm 1, \dots$. On a circle the longitudinal (tangential) and the transversal (radial) displacements are mixed in a way determined by the angle $\theta(q)$. From the definition (30) we see that $\tan(2\theta(q)) = -\tan(2\theta(-q))$. This means that $2\theta(q) = -2\theta(-q)$ or $2\theta(q) = \pi - 2\theta(-q)$. We choose the first relation and, consequently, $\theta(0) = 0$ and $-\pi/2 \leq 2\theta(q) \leq \pi/2$.

According to (32), in a circle with N sites, the phonon Hamiltonian has two normal branches with different q which take N values, i.e. $2N$ frequencies. Note that in a circle with N particles, each of which has two degrees of freedom, the number of normal vibrations is $2N - 3$ because there are two degrees of freedom which correspond to the motion of the centre of mass of the system and one degree corresponds to the rotation of the circle. And indeed, there are three zero frequencies in the vibrational spectrum (32), namely: $\Omega_1(0) = \Omega_2(\pm 2\pi/N) = 0$. At $q = 0$, $\theta(0) = 0$ and the normal coordinate $Q_{1,q=0}$ corresponds to the site displacements $u_n = 1/\sqrt{MN}Q_{1,0}$ and $s_n = 0$, i.e. this is the rotation of the circle. At $q = \pm 2\pi/N = \pm\alpha$ $\theta(\pm\alpha) = \pm\pi/4$, the normal coordinates $Q_{2,\pm\alpha}$ describe the site displacements: $\vec{r}_n = \vec{e}_x\sqrt{2/(MN)}Q_{im2,\alpha}$ and $\vec{r}_n = \vec{e}_y\sqrt{2/(MN)}Q_{re2,\alpha}$ and correspond to the motion of the centre of mass in two mutually orthogonal directions. Here we introduce the notations $Q_{rej,\alpha} = [Q_{j,\alpha} + Q_{j,\alpha}^*]/2$ and $Q_{imj,\alpha} = i[Q_{j,\alpha} - Q_{j,\alpha}^*]/2$ after taking into account the relation $Q_{j,-\alpha} = Q_{j,\alpha}^*$. It is natural that the quasiparticles do not interact with these normal coordinates. From (38) and (39) we see that $F_1(k, 0) = F_2(k, \pm\alpha) = 0$.

For the values $q = 0$ and $q = \pm\alpha$ we have two nonzero frequencies which have no analogue in an open chain. The frequency

$$\Omega_2^2(0) = 4\frac{\kappa}{M}\sin^2\left(\frac{\alpha}{2}\right) \quad (43)$$

is the frequency of the total symmetrical vibration which corresponds to the circle breathing, i.e. to the deviation of the circle radius from its equilibrium value R_0 , because the normal coordinate $Q_{2,q=0}$ describes the site displacements $s_n = 1/\sqrt{MN}Q_{2,0}$ and $u_n = 0$. The doubly degenerate frequency

$$\Omega_1^2(\pm\alpha) = 8\frac{\kappa}{M}\sin^2\left(\frac{\alpha}{2}\right)\cos^2\left(\frac{\alpha}{2}\right)[1 + 4c\sin^2\left(\frac{\alpha}{2}\right)] \quad (44)$$

is the frequency of vibrations which correspond to the nonsymmetrical deformation of the circle into two mutually orthogonal directions. The normal coordinates $Q_{1,\pm\alpha}$ describe the site displacements $\vec{r}_n^{(j)} = \vec{e}_n^{(j)}A_j$ ($j = 1, 2$)

which are characterised by the two mutually orthogonal unit vectors of deformation

$$\vec{e}_n^{(1)} = \vec{e}_x \cos(2n\alpha + \theta_0) - \vec{e}_y \sin(2n\alpha + \theta_0), \quad (45)$$

$$\vec{e}_n^{(2)} = \vec{e}_x \sin(2n\alpha + \theta_0) + \vec{e}_y \cos(2n\alpha + \theta_0), \quad (46)$$

and the amplitudes $A_1 = \sqrt{2/(MN)}Q_{re1,\alpha}$, $A_2 = \sqrt{2/(MN)}Q_{im1,\alpha}$. The interaction of the quasiparticles with these normal coordinates is determined by the coupling functions

$$F_2(k, 0) = 4 \sin\left(\frac{\alpha}{2}\right)(\chi_1 + G_2 \cos(k)), \quad (47)$$

$$F_1(k, \pm\alpha) = \pm 2\sqrt{2}i \sin(\alpha) \left[\chi_1 \cos\left(\frac{\alpha}{2}\right) + \chi_2 \sin\left(\frac{\alpha}{2}\right) + G_2 \cos\left(k \pm \frac{\alpha}{2}\right) \right]. \quad (48)$$

For other frequencies with $q > \alpha$ we have

$$\Omega_{1,2}^2(q) = \frac{1}{2}(\omega_1^2 + \omega_2^2 \mp \sqrt{\Delta^2 + 4f^2}), \quad (49)$$

and the electron-phonon coupling functions F_i (see (38)) in which

$$\cos(\theta(q)) = \frac{1}{\sqrt{2}} \sqrt{1 + \frac{\Delta}{\sqrt{\Delta^2 + 4f^2}}}, \quad (50)$$

$$\sin(\theta(q)) = \frac{\sqrt{2}f}{\sqrt{(\sqrt{\Delta^2 + 4f^2} + \Delta)\sqrt{\Delta^2 + 4f^2}}}, \quad (51)$$

4 Equations in the adiabatic approximation

Next we consider the ground state of the circle with one quasiparticle. We assume that the adiabatic approximation is applicable and that we can choose the wave-function of the ground state in the form

$$|\psi\rangle = U|\psi_e\rangle, \quad (52)$$

where U is the unitary operator of the coherent molecule displacements,

$$|\psi_e(t)\rangle = \sum_n \phi_n(t) B_n^\dagger |0\rangle = \sum_k \psi(k, t) B_k^\dagger |0\rangle, \quad (53)$$

where the functions ϕ_n and $\psi(k)$ satisfy the normalisation condition:

$$\sum_n |\phi_n|^2 = 1, \quad \sum_k |\psi(k)|^2 = 1. \quad (54)$$

Here the functions ϕ_n and $\psi(k)$ are connected by the same unitary transformation from the site representation to the quasimomentum one, (23), as the operators B_n and B_k .

The zero-order adiabatic approximation is equivalent to the semi-classical approach when the molecule displacements and their canonically conjugate momenta are considered as classical ones. Indeed, by computing the mean value of the Hamiltonian over the state (52), which is a functional of ϕ_n , and of the molecule displacements and of their canonically conjugate momenta, we transform the problem to a classical one which involves classical variables instead of operators. In the site representation the Hamiltonian functional then reads as

$$\begin{aligned} \mathcal{H} = & \sum_n \left(\mathcal{E}_0 |\varphi_i|^2 - j (\varphi_i^* \varphi_{i+1} + \varphi_{i+1}^* \varphi_i) + \chi_1 |\varphi_i|^2 (U_n + U_{n-1}) + \chi_2 |\varphi_i|^2 A_n \right. \\ & \left. + G_2 (\varphi_i^* \varphi_{i+1} + \varphi_{i+1}^* \varphi_i) U_n \right) + \mathcal{W}, \end{aligned} \quad (55)$$

where all the variables are c-numbers and \mathcal{W} is the mean value of the phonon Hamiltonian, H_{ph} , *i.e.* of the classical Hamiltonian of harmonic vibrations of the circle. We can also represent this Hamiltonian in the quasimomentum representation

$$\begin{aligned} \mathcal{H} = & \sum_k \mathcal{E}(k) |\psi(k)|^2 + \sum_{j,q} \hbar \Omega_j(q) |\beta_{q,j}|^2 \\ & + \frac{1}{\sqrt{MN}} \sum_{k,q,j} \Phi_j(k,q) \psi^*(k+q) \psi(k) (\beta_{q,j} + \beta_{-q,j}^*), \end{aligned} \quad (56)$$

where the variables $\psi(k)$ and $\beta_{q,j}$ are connected to ϕ_n and the molecule displacements u_i and s_i and their canonically conjugate momenta p_n and q_n by the same canonical unitary transformations (23), (24), (29), (34) as the corresponding operators.

Then we can write down the Hamiltonian equations of motion for these variables. In particular, we get

$$\begin{aligned} p_n &= M \frac{du_i}{dt}, \\ q_n &= M \frac{ds_i}{dt}. \end{aligned} \quad (57)$$

We will restrict our attention to the stationary solutions for which $\phi_n(t) = \exp(-iEt/\hbar)\phi_n$ (or $\psi(k, t) = \exp(-iEt/\hbar)\psi(k)$) and $p_n = q_n = 0$. Performing the variations of (55) with respect to the variables φ_i , u_i and s_i , we obtain the static equations

$$0 = (\mathcal{E}_0 - E)\varphi_i - J(\varphi_{i+1} + \varphi_{i-1}) + \chi_1\varphi_i(U_i + U_{i-1}) + \chi_2\varphi_i A_i + G_2(\varphi_{i+1}U_i + \varphi_{i-1}U_{i-1}), \quad (58)$$

$$0 = \kappa(\cos^2(\frac{\alpha}{2})(2u_i - u_{i+1} - u_{i-1}) + \cos(\frac{\alpha}{2})\sin(\frac{\alpha}{2})(s_{i-1} - s_{i+1})) + \kappa_b(\sin^2(\frac{\alpha}{2})(2u_i - u_{i+2} - u_{i-2}) + \cos(\frac{\alpha}{2})\sin(\frac{\alpha}{2})(2s_{i-1} - 2s_{i+1} + s_{i+2} - s_{i-2})) + (\chi_1 \cos(\frac{\alpha}{2}) + \chi_2 \sin(\frac{\alpha}{2}))(|\varphi_{i-1}|^2 - |\varphi_{i+1}|^2) + G_2 \cos(\frac{\alpha}{2})(\varphi_{i-1}^*\varphi_i + \varphi_i^*\varphi_{i-1} - \varphi_{i+1}^*\varphi_i - \varphi_i^*\varphi_{i+1}), \quad (59)$$

$$0 = \kappa \sin(\frac{\alpha}{2})(\sin(\frac{\alpha}{2})(2s_i + s_{i+1} + s_{i-1}) + \cos(\frac{\alpha}{2})(u_{i+1} - u_{i-1})) + \kappa_b [\cos^2(\frac{\alpha}{2})(6s_i - 4s_{i+1} - 4s_{i-1} + s_{i+2} + s_{i-2}) + \cos(\frac{\alpha}{2})\sin(\frac{\alpha}{2})(2u_{i+1} - 2u_{i-1} + u_{i-2} - u_{i+2})] + 2(\chi_1 \sin(\frac{\alpha}{2}) + \chi_2 \cos(\frac{\alpha}{2}))|\varphi_i|^2 + (\chi_1 \sin(\frac{\alpha}{2}) - \chi_2 \cos(\frac{\alpha}{2}))(|\varphi_{i+1}|^2 + |\varphi_{i-1}|^2) + G_2 \sin(\frac{\alpha}{2})(\varphi_{i-1}^*\varphi_i + \varphi_i^*\varphi_{i-1} + \varphi_{i+1}^*\varphi_i + \varphi_i^*\varphi_{i+1}). \quad (60)$$

Note that the equations (59-60) are invariant under the following transformation:

$$\begin{aligned} u_i &\rightarrow -u_i, \\ s_i &\rightarrow -s_i, \\ \chi_n &\rightarrow -\chi_n \quad (n = 1, 2), \\ G_2 &\rightarrow -G_2. \end{aligned} \quad (61)$$

In the quasimomentum representation this system of equations can be rewritten in the following form

$$(\mathcal{E}(k) - E)\psi(k) + \frac{1}{\sqrt{MN}} \sum_{q,j} F_j(k - q, q)Q_j(q)\psi(k - q) = 0, \quad (62)$$

$$\Omega_j^2(q)Q_j(q) = -\frac{1}{\sqrt{MN}} \sum_k F_j^*(k, q)\psi^*(k)\psi(k + q), \quad (63)$$

where

$$Q_j(q) = \sqrt{\frac{\hbar}{2\Omega_j(q)}}(\beta_{q,j} + \beta_{-q,j}^*). \quad (64)$$

From Eq. (63) we obtain the explicit expressions for $Q_j(q)$, namely:

$$Q_j(q) = -\frac{1}{\sqrt{MN}} \sum_k \frac{F_j^*(k, q)}{\Omega_j^2(q)} \psi^*(k) \psi(k + q). \quad (65)$$

Substituting these expressions into (62), we obtain the following nonlinear integral equation for $\psi(k)$

$$\begin{aligned} & (\mathcal{E}(k) - E) \psi(k) - \frac{1}{N} \sum_{q, k_1 (|q| > \alpha)} G(k, k_1, q) \psi^*(k_1) \psi(k_1 + q) \psi(k - q) \\ & - \frac{1}{N} \sum_{k_1} \mathcal{F}_0(k, k_1) \psi^*(k_1) \psi(k_1) \psi(k) \\ & - \frac{1}{N} \sum_{k_1, q = \pm \alpha} \mathcal{F}_\alpha(k, k_1, q) \psi^*(k_1) \psi(k_1 + q) \psi(k - q) = 0, \end{aligned} \quad (66)$$

where

$$G(k, k_1, q) = \sum_j \frac{F_j(k - q, q) F_j^*(k_1, q)}{M\Omega_j^2(q)}, \quad (67)$$

$$\mathcal{F}_0(k, k_1) = \frac{F_2(k, 0) F_2^*(k_1, 0)}{M\Omega_2^2(0)}, \quad (68)$$

$$\mathcal{F}_\alpha(k, k_1, \alpha) = \frac{F_1(k - \alpha, \alpha) F_1^*(k_1, \alpha)}{M\Omega_1^2(\alpha)}. \quad (69)$$

Taking into account expressions (32) and (38), and then Eqs.(28) and (39), we obtain

$$G(k, k_1, q) = \frac{\chi_2^2}{\kappa_b} + G_1(k, k_1, q), \quad (70)$$

$$\begin{aligned} G_1(k, k_1, q) = \frac{4}{\kappa} \{ & \chi_1^2 \cos^2\left(\frac{q}{2}\right) + \chi_1 G_2 [\cos(k - \frac{q}{2}) + \cos(k_1 + \frac{q}{2})] \\ & + G_2^2 \cos(k - \frac{q}{2}) \cos(k_1 + \frac{q}{2}) \}. \end{aligned} \quad (71)$$

Substituting expressions (43), (44) and (48) into (68) and (69), we get

$$\begin{aligned} \mathcal{F}_0(k, k_1) &= G_1(k, k_1, 0), \\ \mathcal{F}_\alpha(k, k_1, \alpha) &= G_1(k, k_1, \alpha) + \frac{4}{\kappa} \sin\left(\frac{\alpha}{4}\right) f(k, k_1, \alpha), \end{aligned} \quad (72)$$

where $f(k, k_1, \alpha)$ is a function of k and α , the explicit expression of which will be not essential for us.

5 Fully delocalised states

Equations (59-60) or (62-63) always admit a simple solution for all values of the parameters that correspond to a fully delocalised quasiparticle state, *i.e.* for which the quasiparticle is evenly distributed along all the chain: $\varphi_i = 1/(\sqrt{N}) \exp(ik_0 n)$. In the k -representation this solution is fully localised $\psi(k) = \delta_{k, k_0}$. From (63) we see that in this case $Q_j(q) \sim \delta_{q, 0}$ and, therefore, only the normal coordinate $Q_2(0)$ is nonzero. For $j > 0$ the lowest energy state corresponds to the value $k_0 = 0$. Defining

$$\Lambda = E - \mathcal{E}_0 + 2J, \quad (73)$$

this fully delocalised solution for the ground state is given by

$$\begin{aligned} \psi(k) &= \delta_{k, 0} \\ Q_2(0) &= -\frac{1}{\sqrt{MN}} \frac{F_2^*(0, 0)}{\Omega_2^2(0)} = -\sqrt{\frac{M}{N}} \frac{\chi_1 + G_2}{\kappa \sin(\frac{\alpha}{2})} \end{aligned} \quad (74)$$

in the k -representation, and

$$\begin{aligned} \varphi_i &= \frac{1}{N^{1/2}}, \\ u_i &= 0, \\ s_i &= s = -\frac{1}{N\kappa} \frac{\chi_1 + G_2}{\sin \frac{\alpha}{2}} \end{aligned} \quad (75)$$

in the site representation with

$$\Lambda = -\frac{4(\chi_1 + G_2)^2}{N\kappa} = \lambda J. \quad (76)$$

According to (73), $\Lambda = \lambda J$ determines the eigenvalue of Eq. (59) (or (62))

$$E = \mathcal{E}_0 - 2J + \Lambda = \mathcal{E}(0) + \Lambda, \quad (77)$$

where $\mathcal{E}(0) = \mathcal{E}_0 - 2J$ is the lowest energy level (27) of a quasiparticle in the circle.

The total energy of the system is $E_{tot} = E + \mathcal{W}$. For the fully delocalised solution we have $\mathcal{W} = (1/2) \sum_{j,q} \Omega_j^2(q) |Q_j(q)|^2 = (1/2) \Omega_2^2(0) |Q_2(0)|^2$. So, the total energy of the delocalised state is

$$E_{tot} = \mathcal{E}_0 - 2J - \frac{2(\chi_1 + G_2)^2}{N\kappa} = \mathcal{E}(0) - \epsilon J, \quad (78)$$

where ϵ characterises the decrease of energy due to the electron-phonon interaction. Thus, we see that the localised state of a quasiparticle in a circle is characterised by the following values of λ and ϵ

$$\lambda_{del} = -\frac{2g_l}{N}, \quad \epsilon_{del} = \frac{g_l}{N}, \quad (79)$$

with

$$g_l = \frac{2(\chi_1 + G_2)^2}{J\kappa}. \quad (80)$$

In this state all the s_n are the same and all the u_n vanish; *i.e.* the circle radius changes due to the alteration of the distance between sites $U_n = -\frac{2}{N\kappa}(\chi_1 + G_2)$. Note that, in the limit of large N , $\sin \alpha \approx 2\pi/N$ and $\sin \frac{\alpha}{2} \approx \pi/N$. Thus, $s_i = -(\chi_1 + G_2)/(\pi\kappa)$ which is independent of α .

6 Numerical Solutions

The discrete system of equations (59-60) can be solved numerically. As mentioned above, the system always possesses a fully delocalised solution in which the quasiparticle is evenly distributed between the chain sites. But for most values of the parameters, this is not the solution with the lowest energy. In this section, we describe the numerical solutions (we have fixed the following values $J = 1$, $k = 1$ and $k_b = 0.1$).

We have found several regimes of quasiparticle localisation. The quasiparticle can be strongly localised on one or more sites (Fig. 1a), delocalised over most of the chain like (Fig 1c). Moreover, the maximum of $|\varphi_i|^2$ can be located on one site (Fig 1a) or two sites (Fig 1b). Like all the solutions that we have found, these solutions have a reflection symmetry, but in the first case the axis of symmetry passes through a circle site while in the other one, it passes in between two sites.

We would like to point out here that the actual position of the soliton on the chain is completely arbitrary and on each of the solution presented here it was picked up more or less randomly by the relaxation method.

Moreover, one should note that given our choice of signs (for its definition), λ corresponds to the binding energy and so the ground state is the one for which λ is the largest.

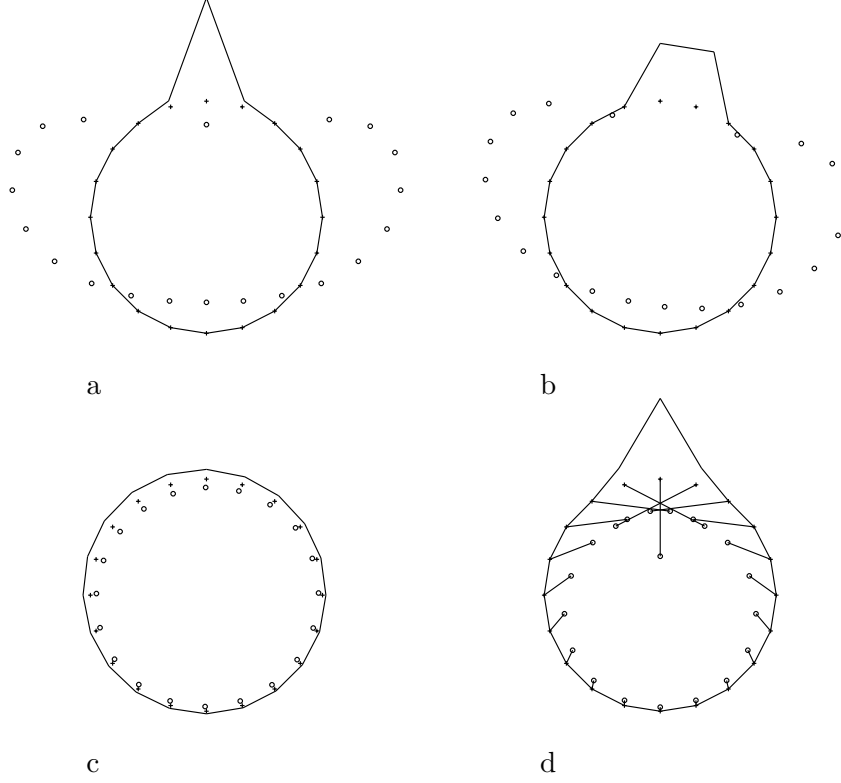


Figure 1: Numerical solutions of Eqs. (59-60) for $G_2 = 1$, $\chi_2 = 0.2$ and a) $\chi_1 = -2$ b) $\chi_1 = -1.5$ c) $\chi_1 = -0.5$ d) $\chi_1 = 2$. Symbols + represent the undeformed chain. Symbols in the form of small circles represent the deformed chain, while the continuous line represents $|\varphi_i|^2$ plotted on the undeformed chain. In d), we also show where each site has been moved to by the chain deformation.

One also notices that the chain can be deformed in different ways. For example, in Figs. 1a and 1b, the chain is pinched into the shape of a bean while in Fig. 1d the chain is compressed with a kink appearing where the soliton is located. The deformation of the chain in all the figures presented here has been scaled in exactly the same way to emphasise the deformation of the chain and show the relative magnitude of the deformation when

the model parameters are varied. The actual amplitude of deformation depends on the values of the parameters and is much smaller than the distance between the chain sites.

Notice also that by virtue of the symmetry (61), the solution in Fig. 1.a can be transformed into a solution for $G_2 = -1$, $\chi_2 = -0.2$ and $\chi_1 = 2$ where, as the sign of u and s changes, the chain is pinched on the sides so that the lattice sites where the soliton is located move outside the circle. By the same symmetry, the solution shown in Fig 1.d is transformed into a ring that is stretched out.

For large values of χ_1 and χ_2 , the solution is usually strongly localised while in the region $\chi_1 = -G_2$, the soliton is fully delocalised. This is shown in Figs. 2-4 where we represent the value of the maximum of $|\varphi_i|^2$ as a function of χ_1 and χ_2 for different values of G_2 .

When $G_2 = 0$, Fig 2, one can see that if $\chi_2 > 0.55$, the soliton is always strongly localised, while for smaller values, the soliton is strongly localised when $\chi_1 \ll 0$. As χ_1 increases, the quasiparticle becomes more and more localised, then it becomes fully delocalised around $\chi_1 = -0.5$. When χ_1 is larger than 0.5, the quasiparticle becomes localised again and it is fully localised as χ_1 goes to ∞ .

At $G_2 = 0.5$, Fig. 3, we see a similar pattern as for $G_2 = 0$ except that the region where the soliton is delocalised is centred around $\chi_1 = -G_2$. For small value of χ_2 , there is also a region where the quasiparticle is delocalised ($-1.5 < \chi_1 < -1$ when $\chi_2 \approx 0$). The solutions in that region are delocalised but have the same symmetry as the fully localised solitons, *i.e.* the axis of symmetry passes through a chain site. In the positive range of χ_1 there is also a region where the quasiparticle is delocalised ($0 < \chi_1 < 1$ when $\chi_2 \approx 0$) but in this case the solution has a different symmetry, *i.e.* $|\varphi_i|^2$ takes its maximum value on two sites and the axis of symmetry passes between two chain sites.

When $G_2 = 1$, Fig 4, we can distinguish 4 different regions. On the outside, the black region corresponds to fully localised solutions (Fig. 1a). On the left, there is a sharp grey region ($-1.8 < \chi_1 < 1$ at $\chi_2 \approx 0$) where the quasiparticle is mostly localised on two neighbouring sites (Fig. 1b). In the white region, the quasiparticle is fully delocalised (Fig. 1c) while in the grey half circle, on the right hand side, the quasiparticle is delocalised with the axis of symmetry passing between two chain sites. Outside this circle the quasiparticle is localised on one site, hence, its symmetry is different (Fig. 1d).

When $G_2 = 1.5$, the structure of the solutions is similar to that of

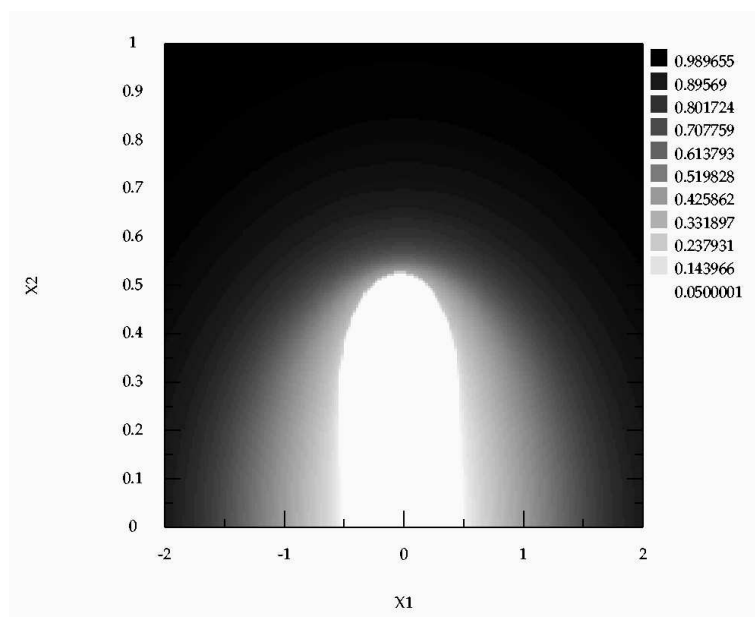


Figure 2: Maximum of $|\varphi_i|^2$ for the solutions of Eqs. (59-60) at $G_2 = 0$. Black corresponds to $|\varphi_i|^2 \approx 1$.

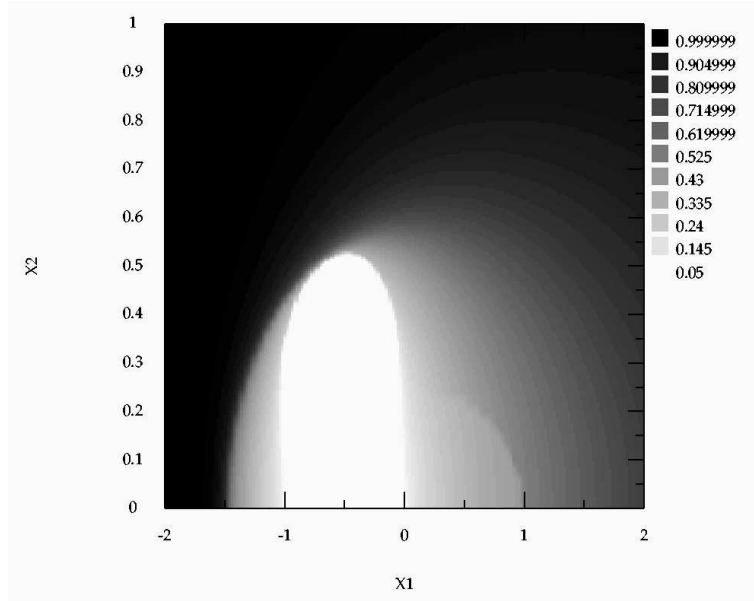


Figure 3: Density of the solutions of Eqs. (59-60), $|\varphi_i|^2$, at $G_2 = 0.5$.

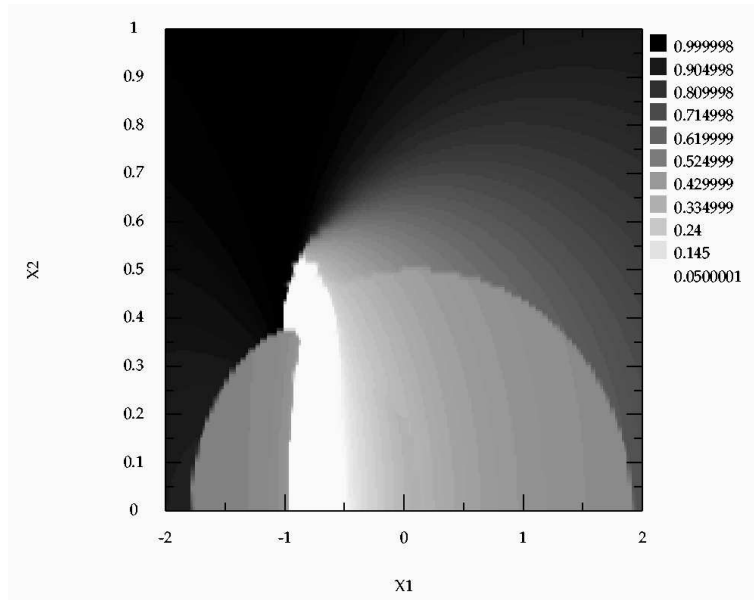


Figure 4: $|\varphi_i|^2$ density for the solutions of (59-60) for $G_2 = 1$.

$G_2 = 1$, but it now exhibits a region where more than one solution exists (other than the fully delocalised solution that always exists). In Fig. 5 we plot the value of $|\varphi_i|^2$ as well as λ as a function of χ_1 and one notices an even richer structure. Notice that λ corresponds to the eigenenergy with opposite sign, so a large value of λ corresponds to a lower energy state.

In Fig. 6 we present several solutions for the same value of $G_2 = 1.5$. When $\chi_1 = -2.7$, Fig.6a, $|\varphi_i|^2 = 0.803$ and the quasiparticle is strongly localised on one site. When $\chi_1 = -2.65$, Fig. 6b, $|\varphi_i|^2 = 0.50$ and the quasiparticle is strongly localised on two neighbouring sites. When $\chi_1 = -0.95$, Fig. 6c and Fig. 6d, there are two solutions, $|\varphi_i|^2 = 0.49$ and $|\varphi_i|^2 = 0.13$. The first one is localised on two sites, while the second one is delocalised and has a different symmetry. Fig. 6b shows that the most localised of these solutions has the lowest energy. When $\chi_1 = 0.05$, $|\varphi_i|^2 = 0.43$, Fig. 6e, *ie* just before the little spike in Fig. 5a, the quasiparticle is slightly delocalised and has a symmetry axis passing through a chain site. When $\chi_1 = 0.1$, $|\varphi_i|^2 = 0.38$, Fig. 6f, *ie* just after the little spike in Fig. 5a, the quasiparticle is still slightly delocalised but it possesses a different symmetry, *ie* the axis of symmetry passes between the 2 chain sites. When $\chi_1 = 2.7$, $|\varphi_i|^2 = 0.48$, Fig. 6g, the quasiparticle is strongly localised on two sites. When $\chi_1 = 2.75$, $|\varphi_i|^2 = 0.714$, Fig. 6h, the quasiparticle is localised on one site.

In Fig. 7 we present the value of $|\lambda|^2$ as a function of G_2 and χ_2 for $\chi_1 = 0$ while Fig. 8 presents some typical solutions for that range of parameters. We notice that when χ_2 and G_2 are small, the quasiparticle is always fully delocalised. When χ_2 is larger than 0.5, there is a triangular region where the solution is strongly localised on one lattice site. We note also that there are 3 different zones with the same shade of grey which we have marked as III, II and 3 in Fig. 7 and which correspond to solutions spread mostly on 3 sites (Fig. 8a and 8b), 2 sites (Fig. 8c and 8d) and 3 sites (Fig. 8e and 8f), respectively.

The most surprising solutions, shown in Fig. 8g and 8h, are non symmetric. They occur when $\chi_2 \geq 0.5$ and when G_2 is large. When G_2 decreases for a fixed value of χ_2 , the asymmetry of the solution decreases so that the solution becomes fully symmetric and the quasiparticle is localised on two sites.

Our numerical solutions show that there are various types of solutions. In particular, they show that if χ_1 , χ_2 and G_2 are not too small, the electron-phonon interaction is responsible for the localisation of the quasiparticle. In particular, a strong interaction between the quasiparticle and the phonon

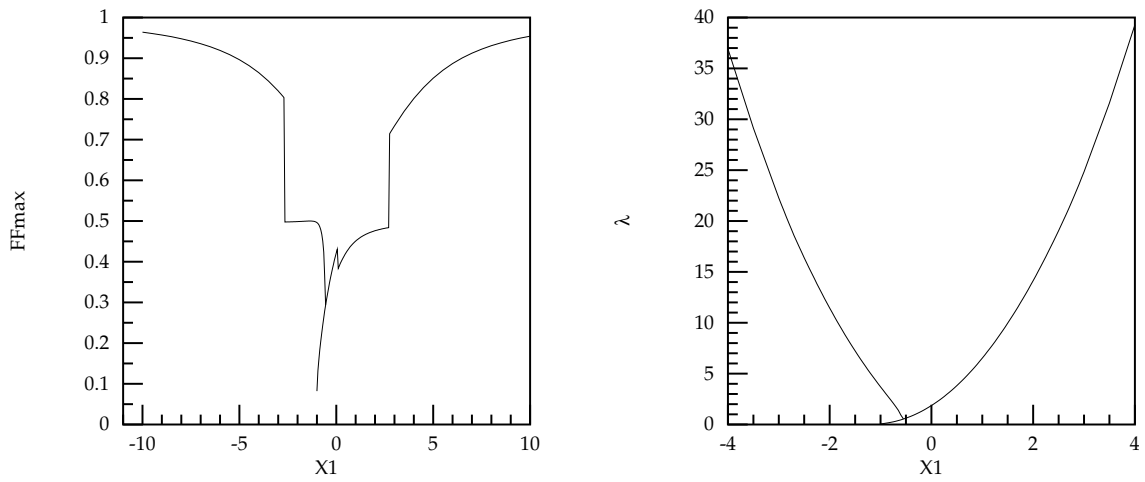


Figure 5: Solutions of Eqs. (59-60) at $G_2 = 1.5$ and $\chi_2 = 0.2$. The plots of:
a) $|\varphi_i|^2$, b) λ .

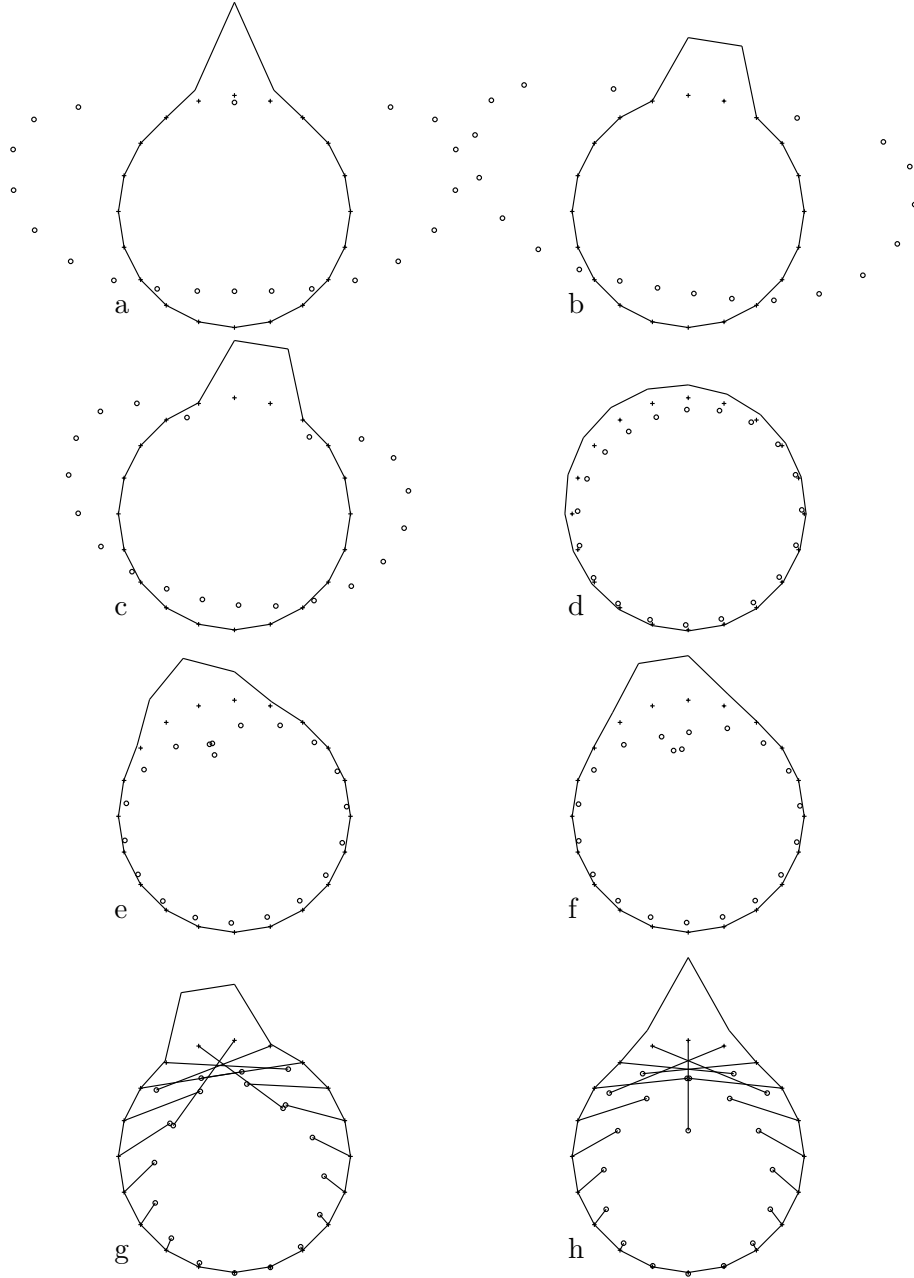


Figure 6: Numerical solutions of Eqs. (59-60) for $G_2 = 1.5$, $\chi_2 = 0.2$ and a) $\chi_1 = -2.7$ b) $\chi_1 = -2.65$ c) $\chi_1 = -0.95$ ($\lambda = 3.38$) d) $\chi_1 = -0.95$ ($\lambda = 0.09$) e) $\chi_1 = 0.05$ f) $\chi_1 = 0.1$ g) $\chi_1 = 2.7$ h) $\chi_1 = 2.75$. The + represent the undeformed chain. Symbols are explained in caption of Fig. 1. In (g) and (h), we also show where each site has been moved to by the chain deformation.

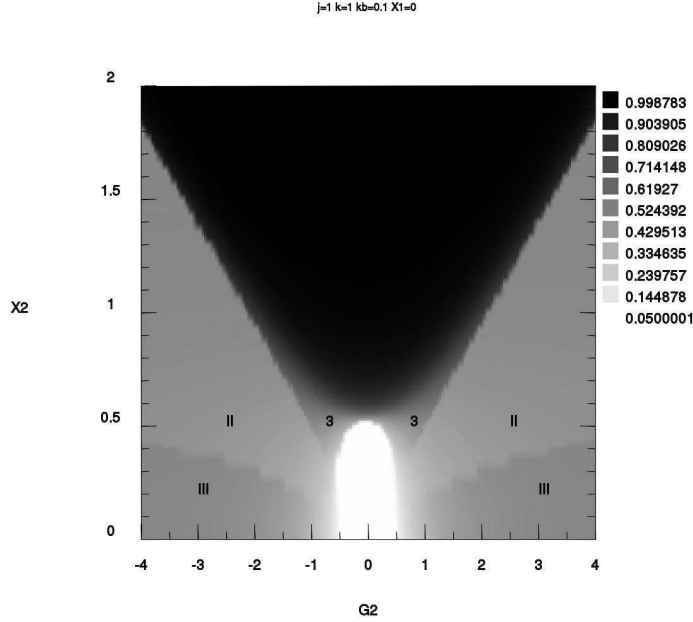


Figure 7: Density for the solutions of Eqs. (59-60), $|\varphi_i|^2$, for $\chi_1 = 0$.

fields (G_2 large) introduces some sharp transition between the different types of solutions and also leads to an overlap between them.

It is also interesting to note that overall, the solution is either localised on a few lattice sites or spread nearly uniformly across the entire chain, but the range of parameters for which a broad soliton exists is very narrow. This is shown on Fig. 2-4 by the sharp transitions between the grey and the white zones.

7 The Continuum Limit.

Though the system of equations always admit localised solutions, these solutions are not always the states of the lowest energy. At strong enough electron-phonon coupling the self-trapping of a quasiparticle can take place with the formation of polaron-type states. Depending on the strength of the coupling, the localisation can be (i) strong with the formation of a small polaron state with the localisation of a quasiparticle mainly on one lattice site, or (ii) comparatively weak with the formation of a large polaron state with the distribution of self-trapped quasiparticle among several lattice sites.

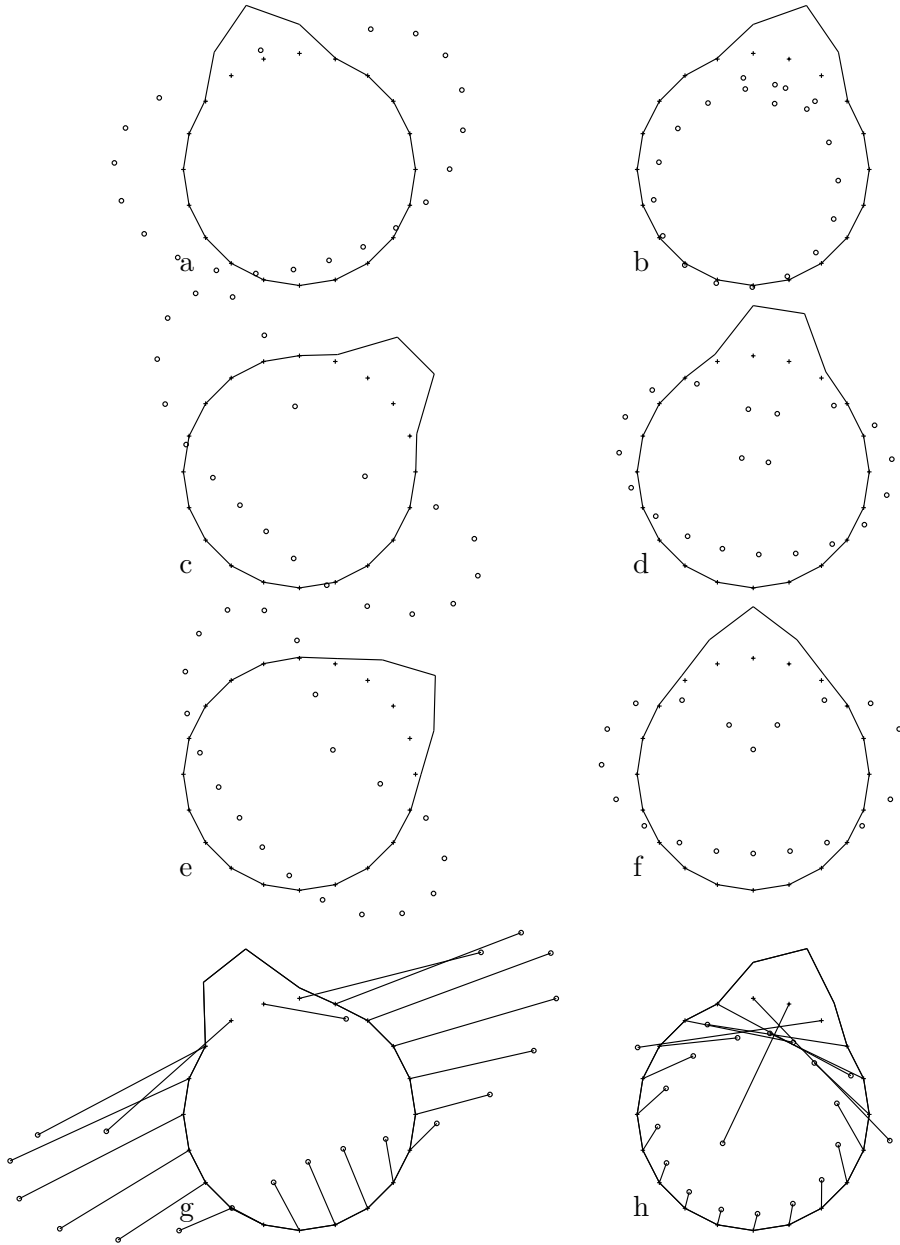


Figure 8: Numerical solutions of Eqs. (59-60) for $\chi_1 = 0$, a) $\chi_2 = 0.1$, $G_2 = -3$ b) $\chi_2 = 0.1$, $G_2 = 3$ c) $\chi_2 = 0.5$, $G_2 = -2$ d) $\chi_2 = 0.5$, $G_2 = 2$ e) $\chi_2 = 0.5$, $G_2 = -0.7$ f) $\chi_2 = 0.5$, $G_2 = 0.7$ g) $\chi_2 = 0.5$, $G_2 = -7$ h) $\chi_2 = 0.5$, $G_2 = 7$ Symbols are explained in caption of Fig. 1. In (g) and (h), we also show to where each site has been moved to by the deformation of the chain.

We consider this latter case here. In linear chains the solutions are well described in the continuum approximation which is valid for large enough systems *i.e.* $N \gg 1$. For a circular chain this means also that α is very small. For such circles, with large enough N , we can neglect the term involving $\sin(\frac{\alpha}{4})$ in (72). In this case Eq. (66) can be rewritten in the form

$$\begin{aligned} (\mathcal{E}(k) - E) \psi(k) - \frac{1}{N} \sum_{q, k_1} G_1(k, k_1, q) \psi^*(k_1) \psi(k_1 + q) \psi(k - q) \\ - \frac{1}{N} \sum_{q, k_1 (|q| > \alpha)} \frac{\chi_2^2}{\kappa_b} \psi^*(k_1) \psi(k_1 + q) \psi(k - q) = 0. \end{aligned} \quad (81)$$

In the last term on the r.h.s. of Eq. (81) we can use the approximation $\sum_{q, k_1, |q| > \alpha} \dots = b^2 \sum_{q, k_1} \dots$. Of course, the value of the constant $b^2 \ll 1$ depends on α as well as on the degree of localisation of the solution. For fully delocalised solutions $b^2 = 0$ but b^2 rapidly tends to unity as the solution becomes more localised. In this way Eq. (81) becomes

$$(\mathcal{E}(k) - E) \psi(k) - \frac{1}{N} \sum_{q, k_1} \tilde{G}(k, k_1, q) \psi^*(k_1) \psi(k_1 + q) \psi(k - q) = 0, \quad (82)$$

where

$$\tilde{G}(k, k_1, q) = b^2 \frac{\chi_2^2}{\kappa_b} + G_1(k, k_1, q). \quad (83)$$

A weak localisation in the site representation corresponds to a strong localisation in the k -representation, *i.e.* $\psi(k)$ ($k = \alpha\nu$) is essentially nonzero only for several values of ν in the vicinity of $\nu = 0$. In the long-wave approximation when $k = \alpha\nu \ll 1$ (which assumes $N \gg 1$) we can write down the following expansions for the functions in (66):

$$\begin{aligned} \mathcal{E}(k) &= \mathcal{E}_0 - 2J + Jk^2 + \dots, \\ G(k, k_1, q) &= b^2 \frac{\chi_2^2}{\kappa_b} + 4 \frac{(\chi_1 + G_2)^2}{\kappa} + \dots \end{aligned} \quad (84)$$

To solve Eq.(66) we introduce the function

$$\varphi(x) = \frac{1}{\sqrt{N}} \sum_k e^{ikx} \psi(k) \quad (85)$$

of the continuum variable x . Note that $\varphi(x)$ is a periodic function, $\varphi(x + N) = \varphi(x)$ and, at $x = n$, this is a unitary transformation of $\psi_\mu(k)$ to the

site representation. Moreover, if $\varphi(x)$ is known, we can find $\psi(k)$.

$$\psi(k) = \frac{1}{\sqrt{N}} \int_{-\frac{N}{2}}^{\frac{N}{2}} e^{-ikx} \varphi(x) dx. \quad (86)$$

Using the approximation (84), one can transform (66) into a nonlinear differential equation for $\varphi(x)$:

$$J \frac{d^2 \varphi(x)}{dx^2} + G |\varphi(x)|^2 \varphi(x) + \Lambda \varphi(x) = 0, \quad (87)$$

which is the stationary nonlinear Schrödinger equation (SNLSE). Here Λ is defined in (73) and

$$G = G(0, 0, 0) = 4 \frac{(\chi_1 + G_2)^2}{\kappa} + \frac{\chi_2^2}{\kappa_b}, \quad (88)$$

Next we rewrite (87) in the dimensionless form after defining

$$\Lambda = -\mu^2 J, \quad \text{and} \quad G = 2Jg \quad \text{where} \quad g = g_l + g_b. \quad g_b = \frac{\chi_2^2}{2J\kappa_b}, \quad (89)$$

where g_l is given in (80). We get

$$\frac{d^2 \varphi(x)}{dx^2} + 2g |\varphi(x)|^2 \varphi(x) - \mu^2 \varphi(x) = 0. \quad (90)$$

We look for a solution of (90) which satisfies the periodic boundary condition

$$\varphi(x + L) = \varphi(x), \quad (91)$$

and the normalisation condition

$$\int_0^L |\varphi(x)|^2 dx = 1, \quad (92)$$

where L is the length of the ring (in the adimensional units used here, $L = N$). We see that $\varphi(x)$ is a real function and so we can integrate Eq.(90) and obtain

$$\left(\frac{d\varphi(x)}{dx} \right)^2 = \mu^2 \varphi^2(x) - g\varphi^4(x) + C \quad (93)$$

where C is the integration constant. So we have to invert

$$x = - \int_{\varphi(0)}^{\varphi(x)} \frac{d\varphi}{\sqrt{\mu^2 \varphi^2 - g\varphi^4 + C}}. \quad (94)$$

Using the substitution

$$\varphi^2 = \frac{1}{g} \left(\frac{\mu^2}{3} - \tau \right), \quad (95)$$

we reduce the problem (94) to a normal Weierstrass form

$$x = \int_{\mathcal{F}(\nu)}^{\mathcal{F}(\xi)} \frac{d\tau}{\sqrt{4\tau^3 - g_2\tau - g_3}} \quad (96)$$

which is solved by the Weierstrass elliptic function $\wp(x + c)$ [20, 21] (c being some constant). Here, and in what follows, we shall use the standard notations for the theory of elliptic functions. In our case, the constants g_2 and g_3 in (96) are determined by

$$\begin{aligned} g_2 &= 4 \left(\frac{1}{3} \mu^4 + gC \right), \\ g_3 &= -\frac{4}{3} \mu^2 \left(\frac{2}{9} \mu^4 + gC \right). \end{aligned} \quad (97)$$

The elliptic Weierstrass function $\wp(z; g_2, g_3) = \wp(z|\omega, \omega')$ is a two-parametric doubly periodic function in the complex plane $z = x + iy$. The two parameters are either the constants g_2 and g_3 or, equivalently, the two periods, which are denoted as 2ω and $2\omega'$, of the function $\wp(z + 2m\omega + 2n\omega') = \wp(z)$ with m and n being integers. In the theory of elliptic functions [20, 21] the following symmetric notations are generally used

$$\omega_1 = \omega, \quad \omega_2 = -\omega - \omega', \quad \omega_3 = \omega' \quad (98)$$

so that $\wp(\omega_j) = e_j$ ($j = 1, 2, 3$) where e_j are the roots of the cubic equation:

$$4\tau^3 - g_2\tau - g_3 = 0. \quad (99)$$

By definition, $|\varphi|^2$ is a real and bounded function of the real coordinate x . Taking into account the analytical properties of the Weierstrass function, we conclude that φ defined by (96) will be physically meaningful only when the discriminant $g_2^3 - 27g_3^2$ of the cubic equation (99) is positive and all three roots e_j are real and different. In the theory of elliptic functions [21] the real roots e_j of the cubic equation (99) are distributed as follows:

$$e_1 > e_2 > e_3 \quad \text{and} \quad e_1 > 0, \quad e_3 < 0. \quad (100)$$

In our case $g_2^3 - 27g_3^2 = 16g^2C^2(\mu^4 + 4gC)$ and the roots of the cubic equation (99) are

$$\frac{1}{3}\mu^2, \quad \frac{1}{2}\left(-\frac{1}{3}\mu^2 \pm \sqrt{\mu^4 + 4gC}\right), \quad (101)$$

i.e. for the integration constant C we have the constraint $4gC \geq -\mu^2$. In this case the period 2ω is real, $2\omega'$ is purely imaginary, and the solution of (96) reads as $\wp(x + \omega')$. Therefore the solution of Eq.(93) (or (94)) is given by

$$\varphi^2(x) = \frac{1}{g}\left(\frac{\mu^2}{3} - \wp(x + \omega')\right). \quad (102)$$

This solution must satisfy the boundary (91) and normalisation (92) conditions which lead to the relations

$$\begin{aligned} 2m\omega &= N, \\ \frac{1}{3}\mu^2 N + 2m\eta &= g. \end{aligned} \quad (103)$$

Here $m = 1, 2, \dots$ is an arbitrary number and $\eta = \zeta(\omega)$ is the constant of the elliptic functions theory ($\zeta(z)$ is the Weierstrass ζ -function determined by the relation $\wp(z) = -\zeta'(z)$). The conditions (103) allow us to determine the integration constant C and the eigenvalue μ^2 , and then to calculate the total energy of the system which includes the energy of the deformation. Using solution (102) we get the following expression for the total energy:

$$E_{tot} = \mathcal{E}(0) - \epsilon J, \quad \epsilon = \frac{1}{3}\mu^2 - \frac{1}{3}CN. \quad (104)$$

To solve the system of equations (103), let us introduce the parameter

$$k^2 = \frac{e_2 - e_3}{e_1 - e_3} \leq 1 \quad (105)$$

which, from now on, will be considered as an independent parameter instead of the integration constant C . Here $e_j = \wp(\omega_j)$ are the roots the cubic equation (99) and k is the modulus of the elliptic Jacobi functions [21]. Using the formulas

$$\mathbf{K}(k) = (e_1 - e_3)^{\frac{1}{2}}\omega, \quad \mathbf{E}(k) = \frac{e_1\omega + \eta}{(e_1 - e_3)^{\frac{1}{2}}}, \quad (106)$$

where $\mathbf{K}(k)$ and $\mathbf{E}(k)$ are complete elliptic integrals of the first and second kind, respectively, we can rewrite the conditions (103) in the form

$$\begin{aligned} 2m\mathbf{K}(k) &= N(e_1 - e_3)^{\frac{1}{2}} \quad , \\ 2m(e_1 - e_3)^{\frac{1}{2}}\mathbf{E}(k) - (e_1 - \frac{1}{3}\mu^2)N &= g. \end{aligned} \quad (107)$$

Inserting the first expression into the second one, we can rewrite (107) as

$$\begin{aligned} 2m\mathbf{K}(k) &= N(e_1 - e_3)^{\frac{1}{2}}, \\ (e_1 - e_3)\mathbf{E}(k) - (e_1 - \frac{1}{3}\mu^2)\mathbf{K}(k) &= \frac{g}{2m}(e_1 - e_3)^{\frac{1}{2}}. \end{aligned} \quad (108)$$

The solution (102) can be rewritten in the form

$$\varphi^2(x) = \frac{1}{g} \left(\left(\frac{\mu^2}{3} - e_3 \right) - \frac{(e_1 - e_3)(e_2 - e_3)}{\wp(x) - e_3} \right). \quad (109)$$

Depending on the sign of the integration constant C , the roots (101) will be enumerated in two different ways according to the rule (100):

$$\begin{aligned} e_1 &= \frac{1}{2}(\sqrt{\mu^4 + 4gC} - \frac{1}{3}\mu^2), \\ e_2 &= \frac{1}{3}\mu^2, \\ e_3 &= -\frac{1}{2}(\sqrt{\mu^4 + 4gC} + \frac{1}{3}\mu^2) \end{aligned} \quad (110)$$

at $C > 0$ and

$$\begin{aligned} e_1 &= \frac{1}{3}\mu^2, \\ e_2 &= \frac{1}{2}(\sqrt{\mu^4 + 4gC} - \frac{1}{3}\mu^2), \\ e_3 &= -\frac{1}{2}(\sqrt{\mu^4 + 4gC} + \frac{1}{3}\mu^2) \end{aligned} \quad (111)$$

at $C < 0$. Two different solutions correspond to these two cases of root distribution.

1) $C > 0$. In this case, taking into account the root distribution (110), we obtain from (105) the following expression for the constant C in terms of k :

$$C = \frac{k^2(1 - k^2)\mu^4}{(2k^2 - 1)^2 g}. \quad (112)$$

The second condition in (108) gives us the expression for μ

$$\mu = \frac{g}{2m} \frac{\sqrt{2k^2 - 1}}{\mathbf{E}(k) - (1 - k^2)\mathbf{K}(k)} \quad (113)$$

and the first one gives us the equation which determines the constant k , the values of which are restricted by the condition that $k > \frac{1}{2}$, namely:

$$\mathbf{K}(k) \left(\mathbf{E}(k) - (1 - k^2)\mathbf{K}(k) \right) = \frac{gN}{(2m)^2} \quad (114)$$

Using the expression for the elliptic Jacobi functions in terms of the Weierstrass function,

$$cn^2(u, k) = \frac{\wp(x) - e_1}{\wp(x) - e_3}, \quad u = (e_1 - e_3)^{1/2} x \quad (115)$$

we find that the solution (109) is given by

$$\varphi(x) = \frac{\sqrt{g}k}{2m[\mathbf{E} - (\mathbf{1} - k^2)\mathbf{K}]} cn \left[\frac{2m\mathbf{K}x}{N}, k \right], \quad (116)$$

From the periodic properties of the function $cn(u, k)$, $cn(u + 4\mathbf{K}, k) = cn(u, k)$, it follows that the periodic condition (91) will be satisfied if $m = 2n$, $n = 1, 2, \dots$. The total energy (104) of the nanocircle in these states is then

$$E_{tot}(n) = \mathcal{E}(0) - \frac{Jg^2}{48n^2} \frac{(2k^2 - 1)\mathbf{E} - (\mathbf{3}k^2 - 1)(1 - k^2)\mathbf{K}}{[\mathbf{E} - (\mathbf{1} - k^2)\mathbf{K}]^3}. \quad (117)$$

2) $C < 0$. In this case the roots are distributed as (111) and from (105) it follows that

$$C = -\frac{1 - k^2}{(2 - k^2)^2} \frac{\mu^4}{g}. \quad (118)$$

The second condition in (108) gives us the expression for μ

$$\mu = \frac{g}{2m} \frac{\sqrt{2 - k^2}}{\mathbf{E}(k)} \quad (119)$$

and the first one gives the equation for determining the constant k

$$\mathbf{E}(k)\mathbf{K}(k) = \frac{gN}{(2m)^2}, \quad (120)$$

Taking into account the relation

$$dn^2(u, k) = \frac{\wp(x) - e_2}{\wp(x) - e_3}, \quad (121)$$

we find that in this case a normalised periodic solution can be expressed in terms of the elliptic Jacobi function as follows:

$$\varphi(x) = \frac{\sqrt{g}}{2m\mathbf{E}(k)} dn \left[\frac{2m\mathbf{K}(k)x}{N}, k \right]. \quad (122)$$

Using the periodic properties of the function $dn(u, k)$, $dn(u + 2\mathbf{K}, k) = dn(u, k)$, it follows that the number m can take the values $m = 1, 2, \dots$. The total energy (104) of the nanocircle in these states is then

$$E_{tot}(m) = \mathcal{E}(0) - \frac{Jg^2}{12m^2} \frac{\mathbf{E}(k)(2 - k^2) + \mathbf{K}(k)(1 - k^2)}{\mathbf{E}^3(k)}. \quad (123)$$

The analysis of Eqs. (117) and (123) shows that the energy of states (122) is always lower than the energy of states (116). Because we are interested in the solutions which correspond to the lowest energy we can ignore the solution (116) and consider only the solution (122). Moreover, we are interested only in the ground state of the circle which corresponds to the value $m = 1$ in (122), (123) and (120). All other states are excited states of the circle.

From (119) and (123) we obtain the following expressions for the eigenvalue

$$\lambda = -\mu^2 = -\frac{g^2}{4} \frac{(2 - k^2)}{E^2(k)}, \quad (124)$$

and for the total energy

$$\epsilon = \frac{g^2}{12} \frac{E(k)(2 - k^2) + K(k)(1 - k^2)}{E^3(k)} \quad (125)$$

of the quasiparticle ground state in the chain.

Let us consider next the case when the modulus of the elliptic function is small, $k^2 \ll 1$, which corresponds to the case of small nonlinearities and not too long chains. In this case, using the expansions of complete elliptic integrals in series of k ,

$$\begin{aligned} \mathbf{K}(k) &= \frac{\pi}{2} \left(1 + \frac{1}{4}k^2 + \frac{3^2}{8^2}k^4 - \dots \right), \\ \mathbf{E}(k) &= \frac{\pi}{2} \left(1 - \frac{1}{4}k^2 - \frac{3}{8^2}k^4 - \dots \right) \end{aligned} \quad (126)$$

we have from (120), at $m = 1$ that

$$k^2 = 4\sqrt{2}\sqrt{\frac{gL}{\pi^2} - 1}. \quad (127)$$

So we can conclude that the solution exists only when g exceeds the critical value of the nonlinearity constant

$$g_{cr}(N) = \frac{\pi^2}{N} \quad (128)$$

which depends on the length of the ring.

In this case the solution (122) can be written as

$$\varphi(x) \approx \frac{\sqrt{g}}{\pi \left(1 - \sqrt{\frac{2gL}{\pi^2} - 2}\right)} \left[1 - 2\sqrt{\frac{2gL}{\pi^2} - 2} \sin^2 \frac{gx}{\pi \left(1 - \sqrt{\frac{2gL}{\pi^2} - 2}\right)} \right] \quad (129)$$

For the eigenvalue and the total energy at $k^2 \ll 1$ expressions (124) and (125) give

$$\lambda_{dn} \approx -\frac{2g^2}{\pi^2} \left(1 + \frac{1}{32}k^4\right), \quad \epsilon_{dn} \approx \frac{g^2}{\pi^2} \left(1 - \frac{1}{32}k^4\right), \quad (130)$$

Remember, that this solution exists only when g exceeds the critical value g_{cr} (128). Below g_{cr} the fully delocalised state is realised on the circle. At $g \rightarrow g_{cr}$ the solution (129) formally tends to a delocalised solution but comparing (79) with (130) shows that even at $g = g_{cr}$ the total energy of the state (122) is lower than energy of the fully delocalised state. Only in the case $g_b = 0$ does the energy of the fully delocalised solution coincide with the energy of the periodic solution at $g = g_{cr}$. At $g > g_{cr}$ the energy of the periodic solution is always lower than the energy of the fully delocalised state.

Let us consider now the opposite case, *i.e.* when the modulus of the elliptic function is close to 1, $k^2 \approx 1$, $k_1^2 = 1 - k^2 \ll 1$. This case, as we will see below, corresponds to long chains and not too small nonlinearity parameters, such that the condition $gN \gg 1$ is satisfied. Then, using the expansion of the elliptic functions and integrals in power series of k_1^2 ,

$$\begin{aligned} \mathbf{K}(k) &= \ln \frac{4}{k_1} + \frac{1}{4} \left(\ln \frac{4}{k_1} - 1 \right) k_1^2 + \dots, \\ \mathbf{E}(k) &= 1 + \frac{1}{2} \left(\ln \frac{4}{k_1} - \frac{1}{2} \right) k_1^2 + \dots, \end{aligned} \quad (131)$$

we get from (120):

$$k_1 = 4e^{-gN/4}, \quad k^2 = 1 - 16e^{-gN/2}. \quad (132)$$

Substituting this into (122), we get

$$\begin{aligned} \varphi(x) \approx & \frac{\sqrt{g}}{2[1 + 2(gN - 2)e^{-gN/2}]} [1 + \\ & + e^{-gN/4} \left(\frac{gx}{2} + \sinh \frac{gx}{2} \cosh \frac{gx}{2} \right) \tanh \frac{gx}{2}] \cosh^{-1} \frac{gx}{2}, \end{aligned} \quad (133)$$

For the eigenenergy and the total energy we get from (124) and (125)

$$\lambda_{dn} \approx -\frac{g^2}{4} \left(1 - 8(2gN - 3)e^{-gN/2} \right), \quad \epsilon_{dn} \approx \frac{g^2}{12} \left(1 + 24e^{-gN/2} \right). \quad (134)$$

We see that at large enough g ($gN \gg 1$) the solution (116) describes a well localised state and that increasing g leads to the increase of the localisation. But it is necessary to keep in mind that the applicability of the continuum approximation is restricted by the condition that the localisation is not too strong which itself imposes the constraint $\mu < \pi/2$.

Using the obtained solution it is possible to calculate the configuration of the circle in the state (116). Taking into account (24), (29), (65), and the explicit expressions for the corresponding functions (32), (38), (39), (28) and (30) we can write

$$u_n = \frac{1}{N} \sum_q e^{iqn} U(q), \quad s_n = \frac{1}{N} \sum_q e^{iqn} S(q), \quad (135)$$

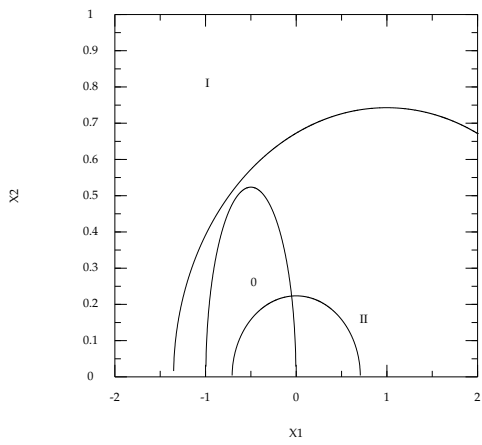
with

$$\begin{aligned} U(q) = & i \sum_k \frac{\frac{\chi_2}{4\kappa_b} \sin(\frac{\alpha}{2}) \cos(\frac{q}{2}) + \cos(\frac{\alpha}{2}) \sin^2(\frac{q}{2}) [\frac{\chi_1}{\kappa} \cos(\frac{q}{2}) + \frac{G_2}{\kappa} \cos(k + \frac{q}{2})]}{\sin(\frac{q}{2}) [\sin^2(\frac{\alpha}{2}) \cos^2(\frac{q}{2}) - \cos^2(\frac{\alpha}{2}) \sin^2(\frac{q}{2})]} \\ & \times \psi^*(k) \psi(k + q), \end{aligned} \quad (136)$$

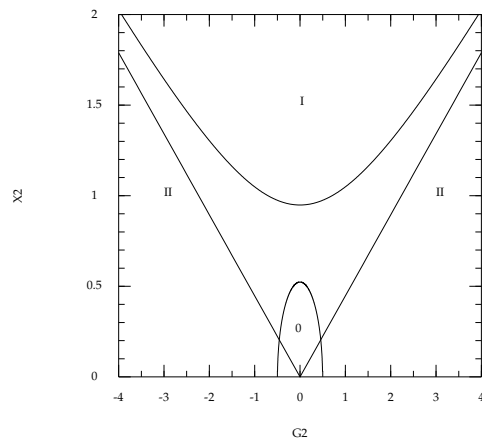
$$S(q) = \sum_k \frac{\frac{\chi_2}{4\kappa_b} \cos(\frac{\alpha}{2}) - \sin(\frac{\alpha}{2}) \cos(\frac{q}{2}) [\frac{\chi_1}{\kappa} \cos(\frac{q}{2}) + \frac{G_2}{\kappa} \cos(k + \frac{q}{2})]}{\sin^2(\frac{\alpha}{2}) \cos^2(\frac{q}{2}) - \cos^2(\frac{\alpha}{2}) \sin^2(\frac{q}{2})} \psi^*(k) \psi(k + q). \quad (137)$$

Here $\psi(k)$ is given by (86) in which $\psi(x)$, in turn, is given by (122).

In Fig. 9 we present the curve of $g = g_{cr} = \pi^2/20$ for $N = 20$, (89), derived in the continuum approximation, where G is given by (84) with



a



b

Figure 9: Regions of solutions: delocalised (0), strongly localised (I) and localised on two adjacent sites (II) for $G_2 = 0.5$ (a) and $\chi_1 = 0.5$ (b)

$b = 0.5$. The curves on Fig. 9 are the two circles of radius 0.5, but which look like vertical ellipses given the different scales of x and y in our plots, enclosing the region marked as '0'. All the solutions inside these circles (marked as 0 in Fig 9) are delocalised. Fig. 9.a corresponds to the case $G_2 = 0.5$ and so can be compared to Fig. 3 obtained numerically, while Fig 9.b corresponds to the case $\chi_1 = 0$ - to be compared with Fig. 7

8 The Limit of Strong Localisation

As we have seen from the discussion above, the increase of the coupling constant reduces the region of localisation of the quasiparticle. Thus, at a large enough value of the coupling the quasiparticle can be localised mostly on one, two, to three lattice sites. In such a case the conditions of the applicability of the continuum approximation are not satisfied. To consider the limit of strong localization, we use Eqs. (71) -(72) to rewrite Eq.(66) as

$$\begin{aligned} (\mathcal{E}(k) - E + \frac{1}{N} \frac{\chi_2^2}{\kappa_b}) \psi(k) + \frac{1}{N} \frac{\chi_2^2}{\kappa_b} [\rho(\alpha) \psi(k - \alpha) + \rho^*(\alpha) \psi(k + \alpha)] \\ - \frac{1}{N} \sum_{q, k_1} G(k, k_1, q) \psi^*(k_1) \psi(k_1 + q) \psi(k - q) = 0. \end{aligned} \quad (138)$$

Here, assuming a large enough circle with $N \gg 1$, we have neglected the term $\sim \sin(\alpha/4)$ in (72). Moreover, we have taken into account the normalization condition (54) and introduced the notation

$$\rho(q) = \sum_k \psi^*(k) \psi(k + q). \quad (139)$$

The function $\psi(k) = (1/\sqrt{N}) \sum_n \exp(-ikn) \phi_n$ is periodic in k , $\psi(k + 2\pi) = \psi(k)$, and so it is representable as a Fourier series

$$\psi(k) = \frac{1}{\sqrt{N}} (c_0 + \sum_{m=1}^{\infty} c_m \cos(mk) + i \sum_{m=1}^{\infty} s_m \sin(mk)). \quad (140)$$

For $\rho(q)$ we then have

$$\rho(q) = c_0^2 + \frac{1}{2} \sum_{m=1}^{\infty} (c_m^2 + s_m^2) \cos(mq) + i \sum_{m=1}^{\infty} c_m s_m \sin(mq) = \rho_r(q) + i \rho_i(q). \quad (141)$$

The coefficients of the expansion satisfy the normalisation condition:

$$\sum_k |\psi(k)|^2 = \rho(0) = c_0^2 + \frac{1}{2} \sum_{m=1}^{\infty} (c_m^2 + s_m^2) = 1. \quad (142)$$

Next we put (140) into (138) and get the Fourier series

$$\{F(0) + \sum_m F(m) \cos(mk) + \sum_m \varphi(m) \sin(mk)\} = 0, \quad (143)$$

thus showing that $F(m) = \varphi(n) = 0$. These conditions give us the equations for c_m and s_n . We have

$$\Lambda_0 c_0 - J_+(0)c_1 - T_-(0)s_1 = 0, \quad (144)$$

$$\Lambda_1 s_1 - \frac{1}{2}J_+(2)s_2 - N_1 c_1 - G_c(0)c_0 - \frac{1}{2}T_-(2)c_2 = 0, \quad (145)$$

$$\Lambda_1 c_1 - J_c(0)c_0 - \frac{1}{2}c_2 - N_1 s_1 - \frac{1}{2}T_-(2)s_2 = 0, \quad (146)$$

$$\begin{aligned} \Lambda_m c_m &- \frac{1}{2}J_-(m-1)c_{m-1} - \frac{1}{2}J_+(m+1)c_{m+1} - N_m s_m \\ &- \frac{1}{2}T_+(m-1)s_{m-1} - \frac{1}{2}T_-(m+1)s_{m+1} = 0, \end{aligned} \quad (147)$$

$$\begin{aligned} \Lambda_m s_m &- \frac{1}{2}J_-(m-1)s_{m-1} - \frac{1}{2}J_+(m+1)s_{m+1} - N_m c_m \\ &- \frac{1}{2}T_+(m-1)c_{m-1} - \frac{1}{2}T_-(m+1)c_{m+1} = 0. \end{aligned} \quad (148)$$

The functions Λ_k , $J_{\pm}(i)$, $T_{\pm}(j)$, N_m , $J_c(0)$ and $G_c(0)$ are functions of s_m and c_n and so we see that we have nonlinear equations for s_k and c_i .

Note that when we have a fully delocalised system all c_k are the same; the same is true of s_k . As the coupling constant increases, s_n become different from each other; in fact, as n increases, they become exponentially small (as a function of n). The same is true also for c_n . Thus, to get an approximate solution, we can take into account only a finite number of s_i and c_i .

Our system of equations (146) always allows us to put $s_n = 0$ and $c_n \neq 0$. If we now assume that $c_2 \ll c_1 < c_0$, we can consider the equations involving only c_0 and c_1 . In this case we have

$$\begin{aligned} &\{\Lambda - (\frac{\chi_2^2}{\kappa_b} + \frac{2\chi_1^2}{\kappa})c_0^2 - \frac{\chi_1^2}{2\kappa}c_1^2 - \frac{8\chi_1 G_2}{\pi\kappa}c_0 c_1\}c_0 \\ &- \{J + \frac{G_2^2}{\kappa}c_0 c_1 + \frac{4\chi_1 G_2}{\pi\kappa}(c_0^2 + \frac{1}{6})\}c_1 = 0, \end{aligned} \quad (149)$$

$$\begin{aligned} & \left\{ \Lambda - \left(\frac{\chi_2^2}{\kappa_b} + \frac{2\chi_1^2}{\kappa} \right) \frac{c_1^2}{4} - \frac{\chi_1^2}{\kappa} c_0^2 - \frac{8\chi_1 G_2}{3\pi\kappa} c_0 c_1 \right\} c_1 - \\ & - \left\{ 2J + \frac{2G_2^2}{\kappa} c_0 c_1 + \frac{8\chi_1 G_2}{\pi\kappa} \left(c_0^2 + \frac{1}{6} \right) \right\} c_0 = 0, \end{aligned} \quad (150)$$

where $\Lambda = \mathcal{E}_0 - E$.

When $c_1 < c_0$ then c_0 and c_1 are given by

$$c_1^2 = \frac{(1 + g_3)(D - g_1 + g_2)}{D + g_3(2D + g_1 - g_2)}, \quad (151)$$

$$c_0^2 = \frac{(1 + 3g_3)(D + g_1 - g_2)}{2[D + g_3(2D + g_1 - g_2)]}, \quad (152)$$

where $g_1 = \frac{\chi_2^2}{\kappa_b J} + \frac{2\chi_1^2}{\kappa J}$, $g_2 = \frac{\chi_1^2}{\kappa J} + \frac{2G_2^2}{\kappa J}$, $g_3 = 4\frac{\chi_1 G_2}{\pi\kappa J}$. Here D is given by

$$D = \sqrt{(g_1 - g_2)^2 + 8(1 + g_3)(1 + 3g_3)}. \quad (153)$$

The quasiparticle wavefunction is now given by

$$\psi_n = c_0 \delta_{n,n_0} + \frac{1}{2} c_1 (\delta_{n,n_0+1} + \delta_{n,n_0-1}), \quad (154)$$

and describes the localisation of the quasiparticle on at most 3 sites .

The energy of this state is given by $E = \mathcal{E}_0 - \frac{1}{2}\{g_1 + g_2 + D\}$. Of course, our expression is valid when $c_1 < c_0$.

In Fig. 9 we present the plots of the curve corresponding to $\frac{c_1^2}{c_0^2} = 0.2$ obtained from (151), (152) and (153). In Fig. 9.a we present the case $G_2 = 0.5$ as a function of χ_1 and χ_2 while Fig. 9.b corresponds to the case $\chi_1 = 0$ as a function of χ_2 and G_2 . Thus, our plots shows the curves which separate the regions of strongly localised solutions from the region where the quasiparticle is localised on a few adjacent lattice sites. The curves are the ones that delimit the region marked as *I* in the figure and which corresponds to the strongly localised solutions. When we compare Fig. 9.a and Fig. 9.b with Fig. 3 and Fig. 7, respectively, we note a very good agreement between our numerical results and our analytical results.

Finally, we consider the case where the quasiparticle is restricted to two neighbouring sites. In this case we consider equations for c_0 , c_1 and s_1 assuming that all other s_i and c_i are negligeably small. Thus, $c_2 = O(\epsilon^2)$ and so is s_2 .

In this case the equations are somewhat complicated, so here we present only their solutions. They are given by:

$$c_1 = c_0 + O(\epsilon^2), \quad s_1 = c_0 - O(\epsilon^2). \quad (155)$$

The condition of normalisation gives us $c_0 \sim \frac{1}{\sqrt{2}}$. The quasiparticle wavefunction is then given by

$$\psi_n = \left(\frac{1}{\sqrt{2}} - O(\epsilon^2) \right) (\delta_{n,n_0} + \delta_{n,n_0+1}). \quad (156)$$

The energy expression is now given by

$$E = \mathcal{E}_0 - J - \frac{1}{2}(g_1 + g_2) + 2g_3. \quad (157)$$

Our numerical calculations, see Fig. 6c and d, have shown that at the same values of the parameters we can have two different solutions, one localised essentially on two sites and the other localised over a larger number of sites. These two solutions have different energies.

The necessary condition for the existence of solutions localised on two adjacent lattice sites is that $g_1 - g_2$ satisfies the relation

$$g_2 - g_1 = \frac{2G_2^2}{\kappa J} - \left(\frac{\chi_2^2}{\kappa_b J} + \frac{\chi_1^2}{\kappa J} \right) > 0. \quad (158)$$

The physically relevant solution is, of course, given by the state which has the lowest energy. The two site solution has the lowest energy when G_2 is significantly larger than all other parameters.

In Fig. 9 we present the curve $g_2 - g_1 = 0$ corresponding to the limit of a solution localised on two adjacent sites. Fig. 9.a presents the case of $G_2 = 0.5$ as a function of χ_1 and χ_2 and the curve is the ellipse, appearing as a circle on our scale, near the symbol 'II'. The solutions localised on two sites exist just outside the ellipsoidal region marked as *II*. Note also that in the region contained in the intersection between region 0 and region *II*, the solutions are delocalised. All this confirms the numerical results displayed in Fig. 3.

Fig. 9.b presents the case $\chi_1 = 0$ as a function of χ_2 and G_2 . The curves are the two straight lines and the solutions localised on two sites exist in the region marked as *II*, just below the two lines. This is also in very good agreement with Fig. 7.

Notice also that we do not have any theoretical prediction for the transition from solutions localised on two sites to those localised on three sites.

For the case $G_2 = 0$, Eq. (158) has no solution and so there are no solutions localised on two neighbouring sites in that case, confirming our numerical results.

We should point out that we have also computed the theoretical predictions for the different types of solutions corresponding to the case $G_2 = 0$ and $G_2 = 1$. When we have compared these predictions to the numerical results presented in Fig. 2 and Fig. 4 we have also found a very good agreement.

9 Conclusions

We have shown that one can successfully describe the electron-phonon interaction of a circular chain while taking into account the transversal and longitudinal displacement of the ring of monomers. To achieve this, we have introduced a term in the phonon Hamiltonian which describes the bending of the chain. This extra displacement can, in turn, be coupled to the quasiparticle and this coupling favours a self-trapping of quasiparticles and the formation of localised soliton-like structures.

The transversal displacement plays an important role in the formation of such states. The interaction between the quasiparticle and the phonon field leads not only to the localisation of the quasiparticle but also to a deformation of the circle. Depending on the coupling between the two fields, the circle is pinched at the position of the soliton or on the either side of it.

We have studied our model by solving its classical equations numerically. Our numerical studies have shown a great richness of solutions; hence we have also tried to solve our equations analytically. To do this we have had to perform several approximations. We have found that, at least in the regions of validities of these approximations, our analytical results are in good agreement with our numerical results.

Our results show that, depending of the choice of the parameters, our model possesses several classes of solutions. Fully delocalised solutions exist for all values of the parameters. They do not correspond to the ground state when other solutions exist but they are the only solutions when the parameters $\chi_1 + G_2$ and χ_2 are small. On the other hand, strongly localised solutions exist when the coupling parameters are large. For these solutions, the quasiparticle is localised mostly on one lattice site, but the

circle is completely distorted, *i.e.* the strong localisation applies only to the quasiparticle, not the displacement fields.

We also found some solutions that are localised on two adjacent sites and have a different symmetry.

Our study has shown that the electron-phonon interaction on a circular chain leads to the formation of bound states and to the deformation of the chain. Our results can be used to the description of various systems mentioned in the introduction and as a ‘warm-up’ stage to the description of various 3-dimensional systems such as *e.g.* nanotubes.

10 Acknowledgement

This work has been supported by a Royal Society travel grant. We would like to thank Yu. Gaididei for his interest and helpful discussions.

References

- [1] B. Hartmann, W.J. Zakrzewski, Phys.Rev. **B68**, 184302 (2003).
- [2] L. Stryer, Biochemistry, W.H. Freeman, Inc., 1981.
- [3] C.E. Swenberg, E.A. Holwitt, J.M. Speicher, SAE Technical Paper Series, No. 901349, 20th Intersociety Conference on Environmental Systems, Williamsburg, Virginia, July 9-12, 1990, pp. 1-7.
- [4] C.J. Benham, Comments Mol. Cell. Biophys., v. 4, 1986, 35-53.
- [5] T.J. Worst, W.M. Freeman, S.J. Walker, K.E. Vrana, Methods Mol Med., 2003, 79:243-59.
- [6] CF Bleczinski, C. Richert, Org Lett. 2000 Jun 15;2(12):1697-700.
- [7] N.C. Seeman, H. Wang, X. Yang, F. Liu, et al. Phiset Sa-Ardyen, Bing Liu, Hangxia Qiu, New Motifs In DNA Nanotechnology. Proceedings of the Fifth Foresight Conference on Molecular Nanotechnology.
- [8] A.J. Zaug, P.J. Grabowski, T.R. Sech, Nature, 1983, v. 301, 578;
- [9] T.R. Sech, Annu. Rev. Biochem, 1990, v. 59, 543.

- [10] P. Ross, H. Weinhouse, Y. Aloni, D. Michaeli, P. Weinberger-Ohama, R. Mayer, S. Braun, E. de Vroom, G.A. van der Marel, J.H. van Bloom and M. Benziman, *Nature*, 1987, v. 325, 279.
- [11] C.-Y. Hsu, D. Dennis, *Nucleic Acids Res.*, 1982, v. 10, 5637.
- [12] E. Allazzouzi, N. Escaja, A. Grandas, E. Pedroso, *Angew. Chem., Int. Ed. Engl.*, 1997, v. 36, 1506.
- [13] M. Frieden, A. Grandas, F. Pedroso, *Chem. Commun.*, 1999, 1593-1594
- [14] <http://fred.hmc.psu.edu/ds/retrieve/fred/meshdescriptor/D017362>
- [15] M.D. Michael, M.W. Kilgore, K. Morohashi, E.R. Simpson, *J. Biol. Chem.* 1995 Jun 2;270(22):13561-6.
- [16] J.E. Mark, H.R. Allock, R. West, *Inorganic Polymers*, (Prentis Hall advanced reference series. Physical and life sciences) (Polymer science and engineering series) Prentis Hall, Inc., New Jersey, 1992.
- [17] L.S. Brizhik, A.A. Eremko, *Z. Phys. B*, 1997, V. 104, 771-775.
- [18] L.S. Brizhik, K. Dichtel, A.A. Eremko, *J. Superconductivity*, 1999, V.12, 339-341.
- [19] L.S. Brizhik, A.A. Eremko, *Synth. Met.*, 2000, v. 109, No 1-3, 117-121.
- [20] N.I. Akhiezer, *Elementy Teorii Ellipticheskikh Funktsiy* (Nauka, Moscow, 1970).
- [21] H. Bateman and A. Erdélyi, *Higher Transcendental Functions* (McGraw-Hill, New York, 1955), Vol.3.